Building a Hybrid Compton Camera System for Improving Medical Imaging Applications
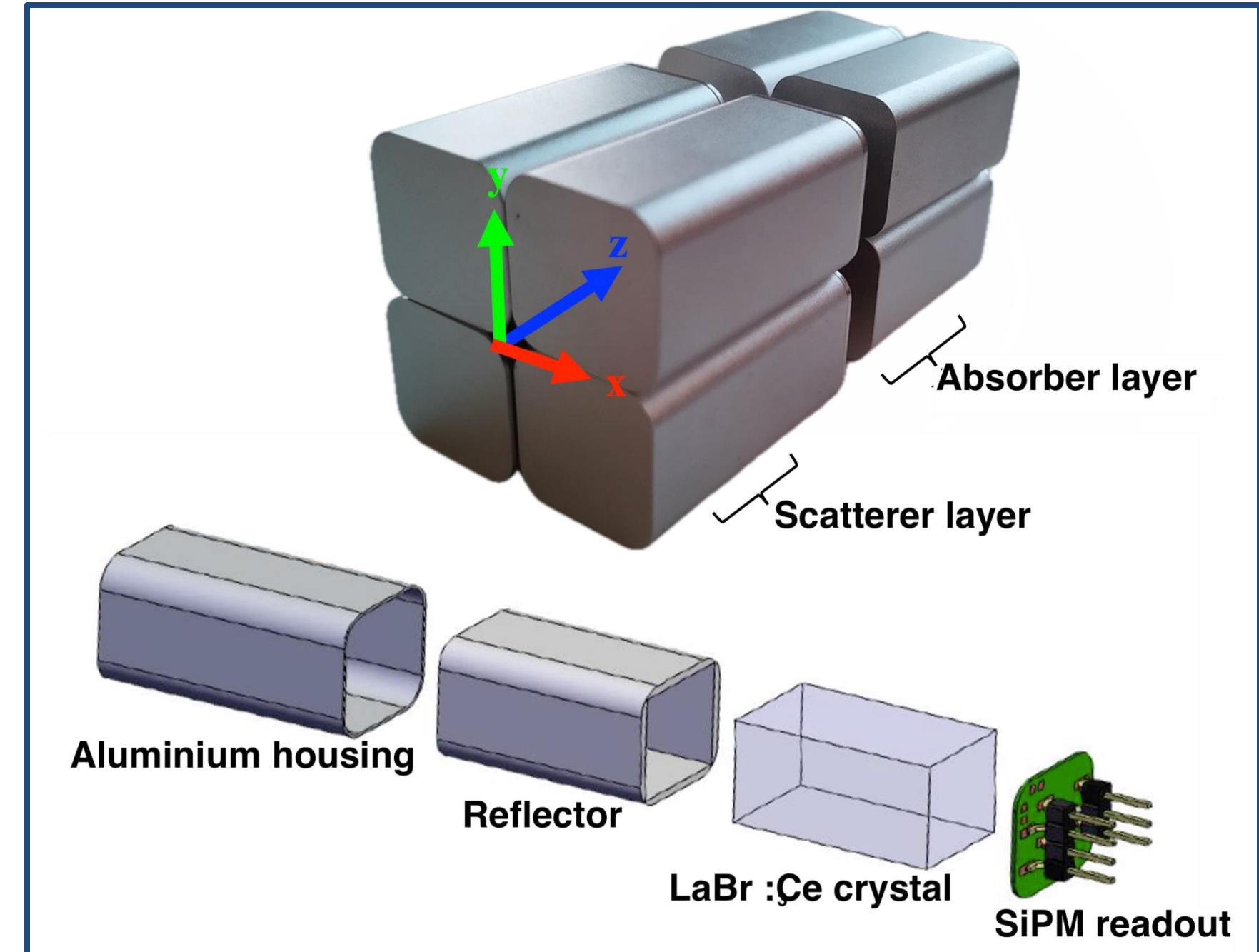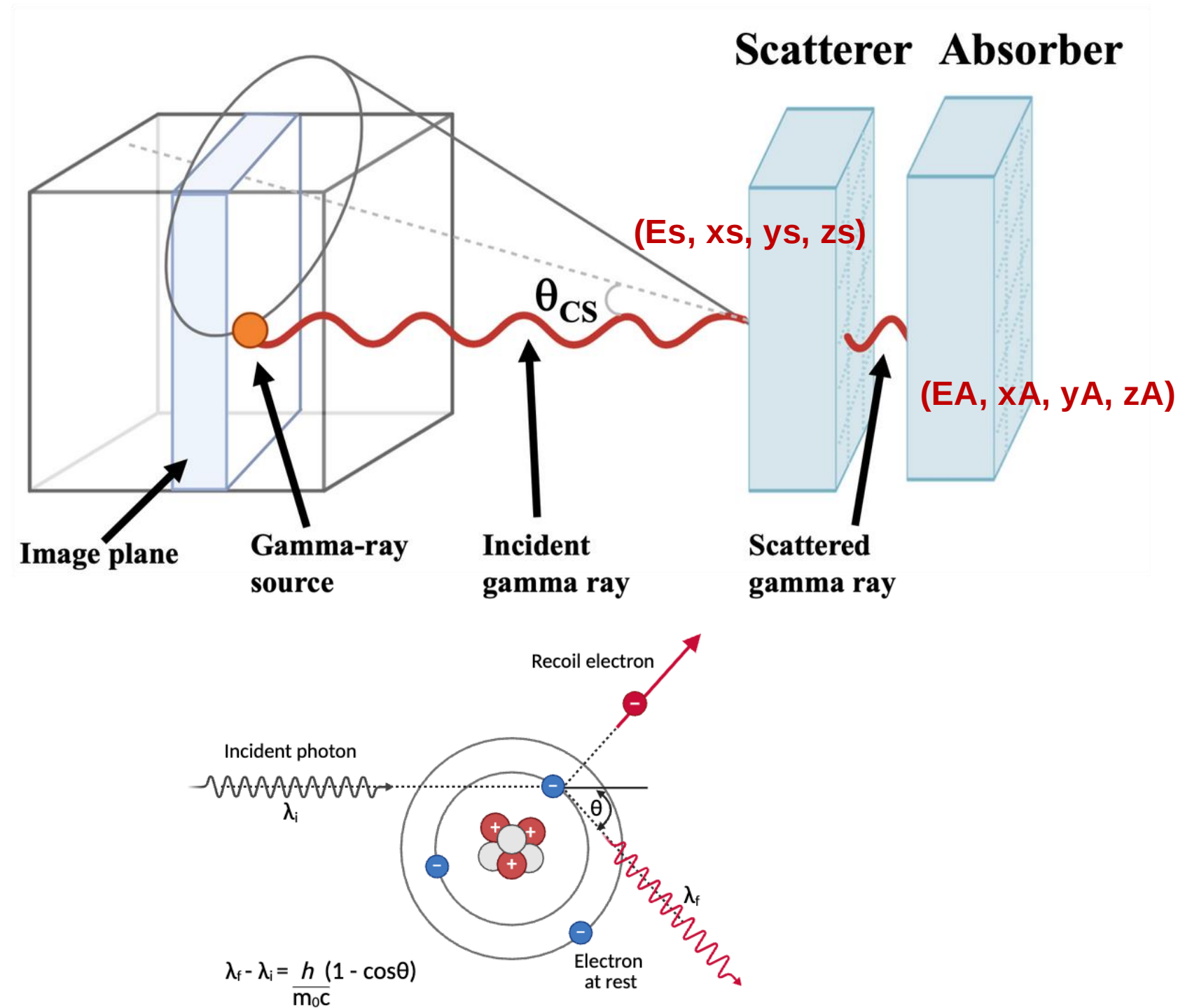
Shanyn Hart, Postdoctoral Researcher at iThemba LABS

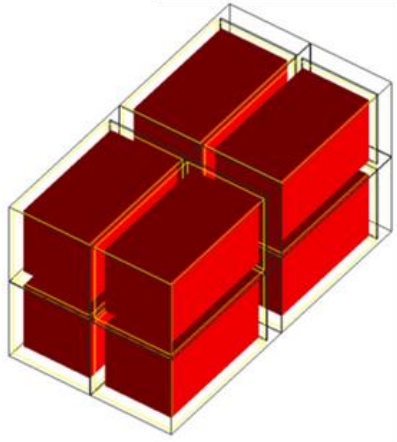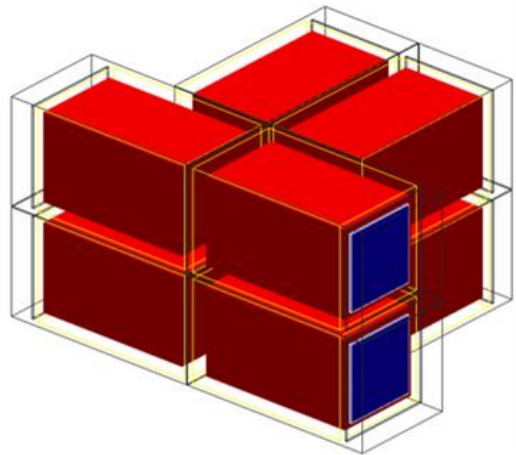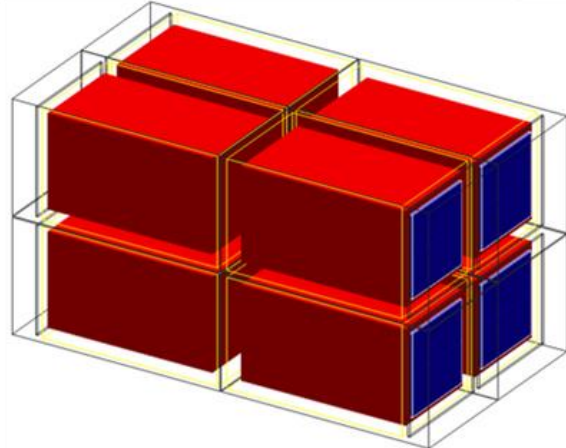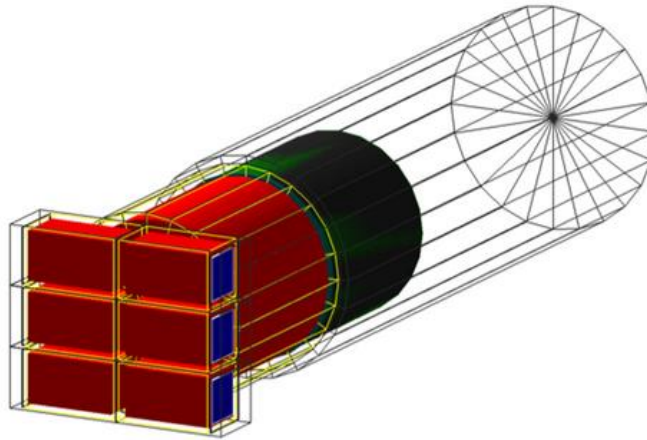**ANPC 2025**

Compton Camera Principle

Scatterer and Absorber Layers:
MacroPixel LB-14x25c-SiPM-T LaBr$_3$:Ce detector assemblies in 4 × 1 arrays.

Compton Camera Geometries Investigated
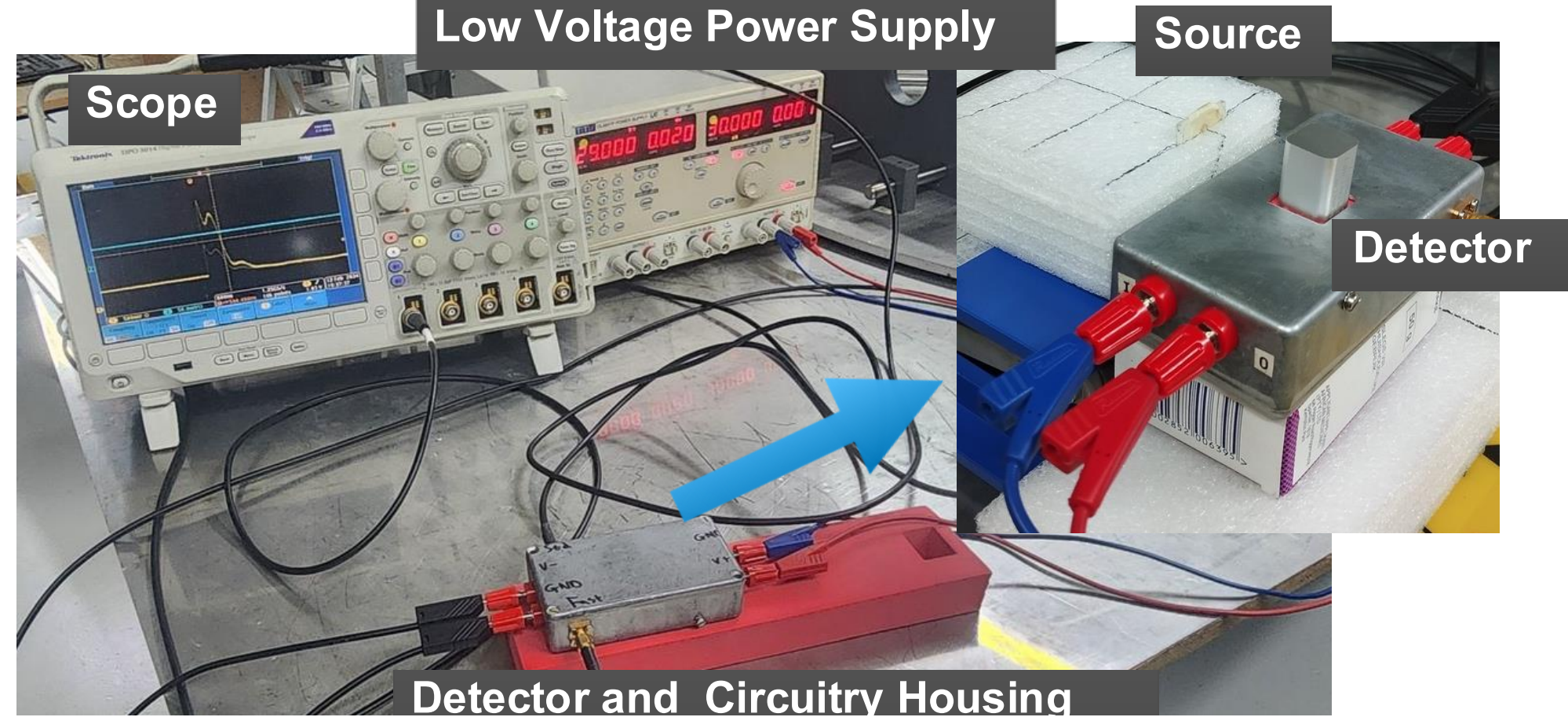

Scatterer	LaBr$_3$:Ce DA	LaBr$_3$:Ce DA	LaBr$_3$:Ce DA	LaBr$_3$:Ce DA
Absorber	LaBr$_3$:Ce DA	LaBr$_3$:Ce DA	LaBr$_3$:Ce DA	2"x2" LaBr$_3$:Ce

I will discuss this design.

CC Detector Characterisation

Compton Camera of **LaBr₃:Ce** OR **SrI2:Eu** detectors (14 x 14 x 25.4 mm³) coupled to a **2x2 MicroFJ-60035-TSV SiPM** array and **TMP451** temperature sensor packed in an aluminium canister. Manufactured by **CapeScint** (MA,USA).

Low Voltage Power Supply

Source

Scope

Detector

Detector and Circuitry Housing

Slow

V-

Ground

Ground

V+

Fast

χ^2/ndf 30.6/17
p0 $-3.82 +/- 3.10$
p1 $28.40 +/- 1.84$
p2 $7.47 +/- 0.25$

1173.2 keV ^{60}Co

1173.2 keV

1332.5 keV
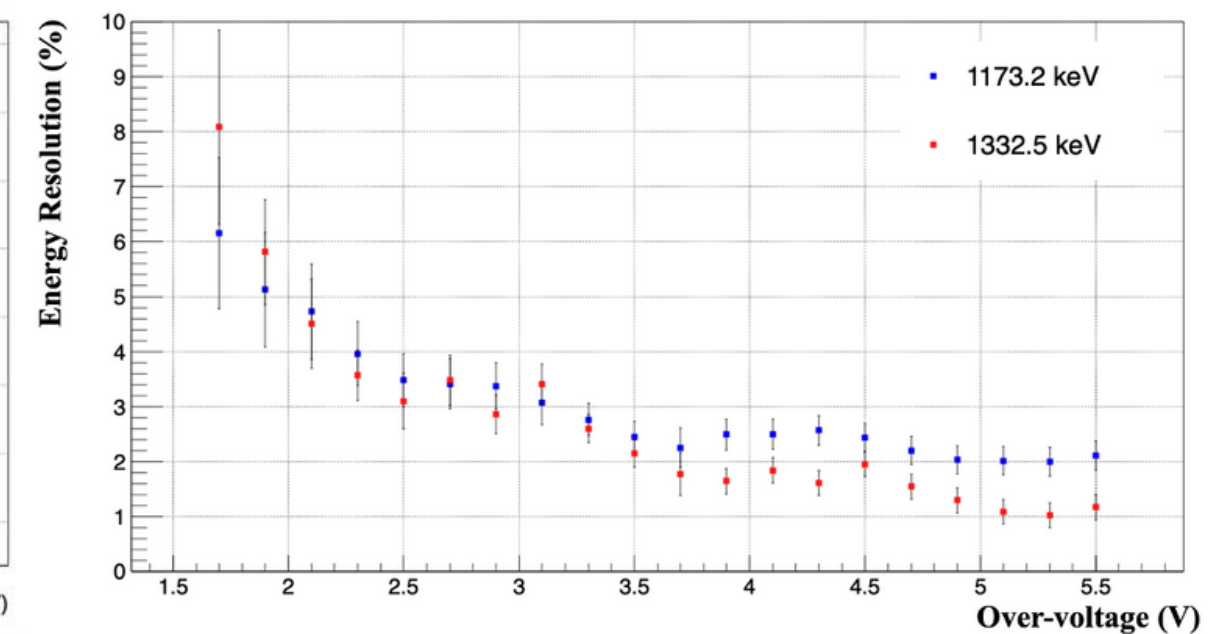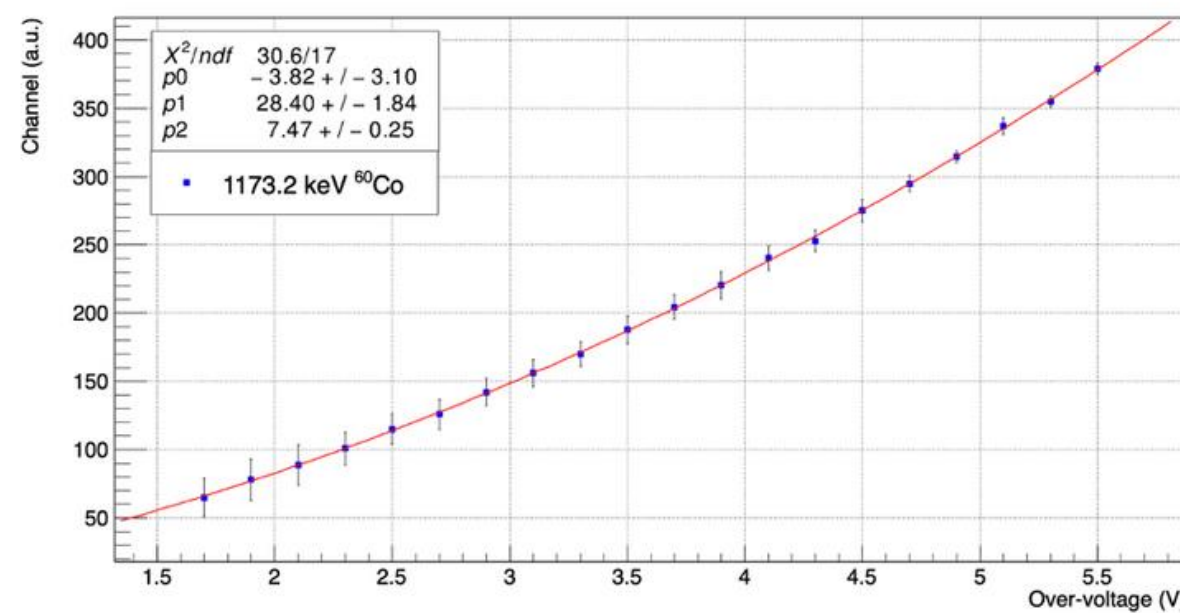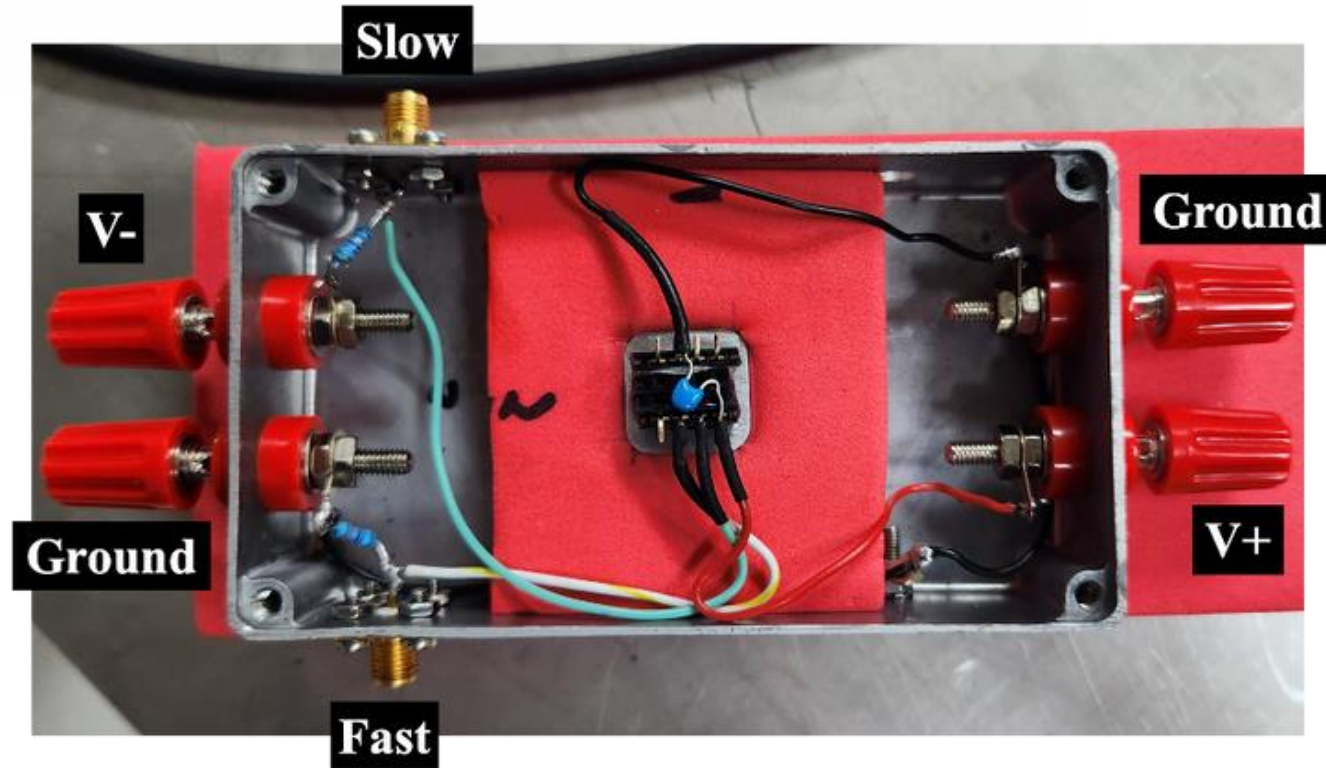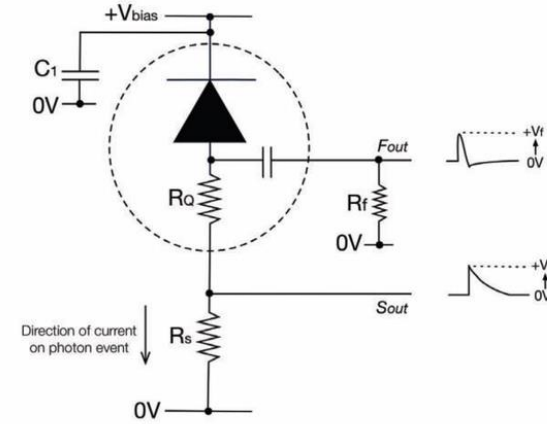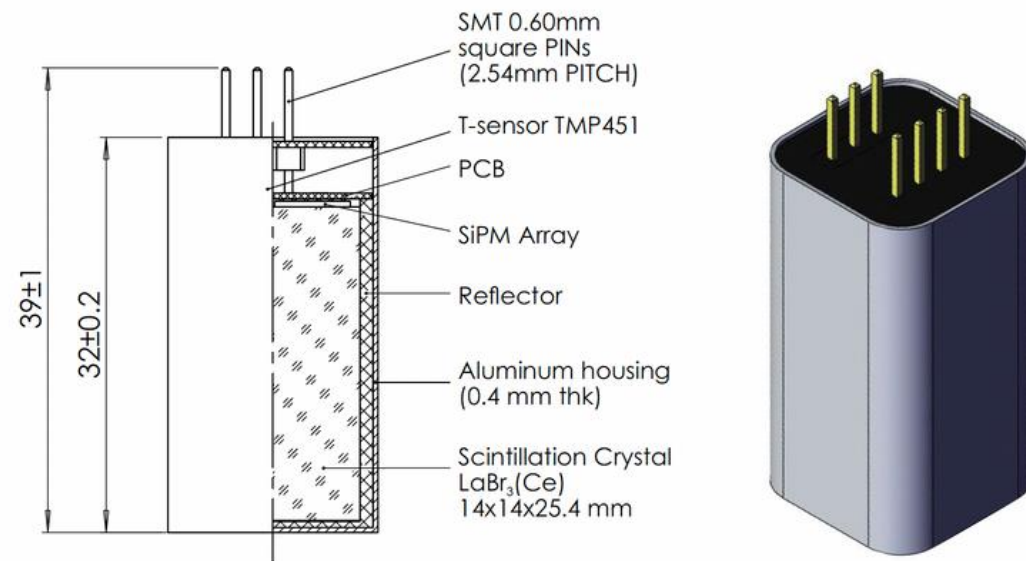
Operational voltage chosen to be 30 V (5.3 V overvoltage)

Validation of CC Detector Simulation

LaBr$_3$:Ce-SiPM

^{152}Eu

$$R(E) = \frac{59.41(1291)}{\sqrt{E}} + 1.31(46)$$

$$\chi^2/NDF = 0.16$$

Energy resolution smearing

High efficiency for Compton scattering at low energies. Good candidate for addback.
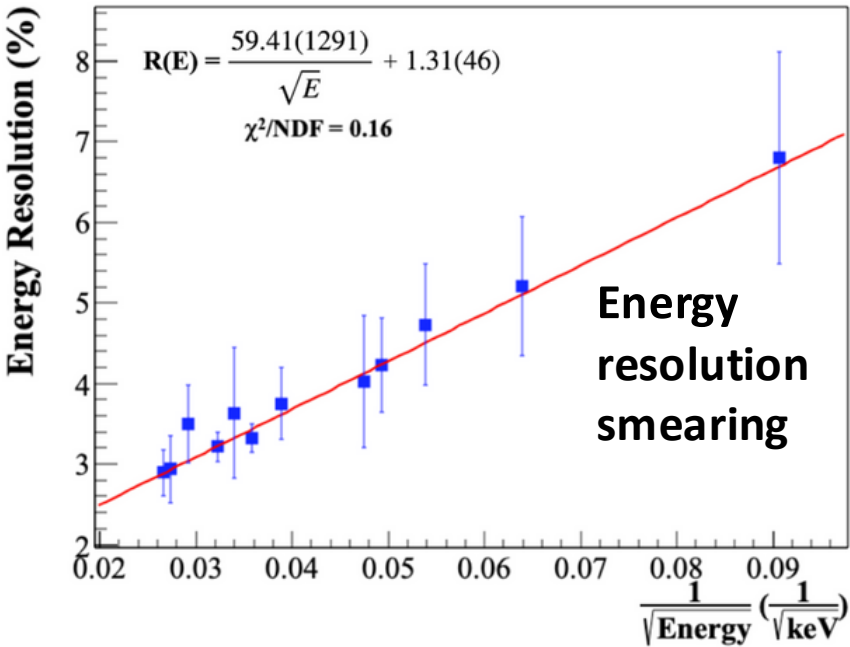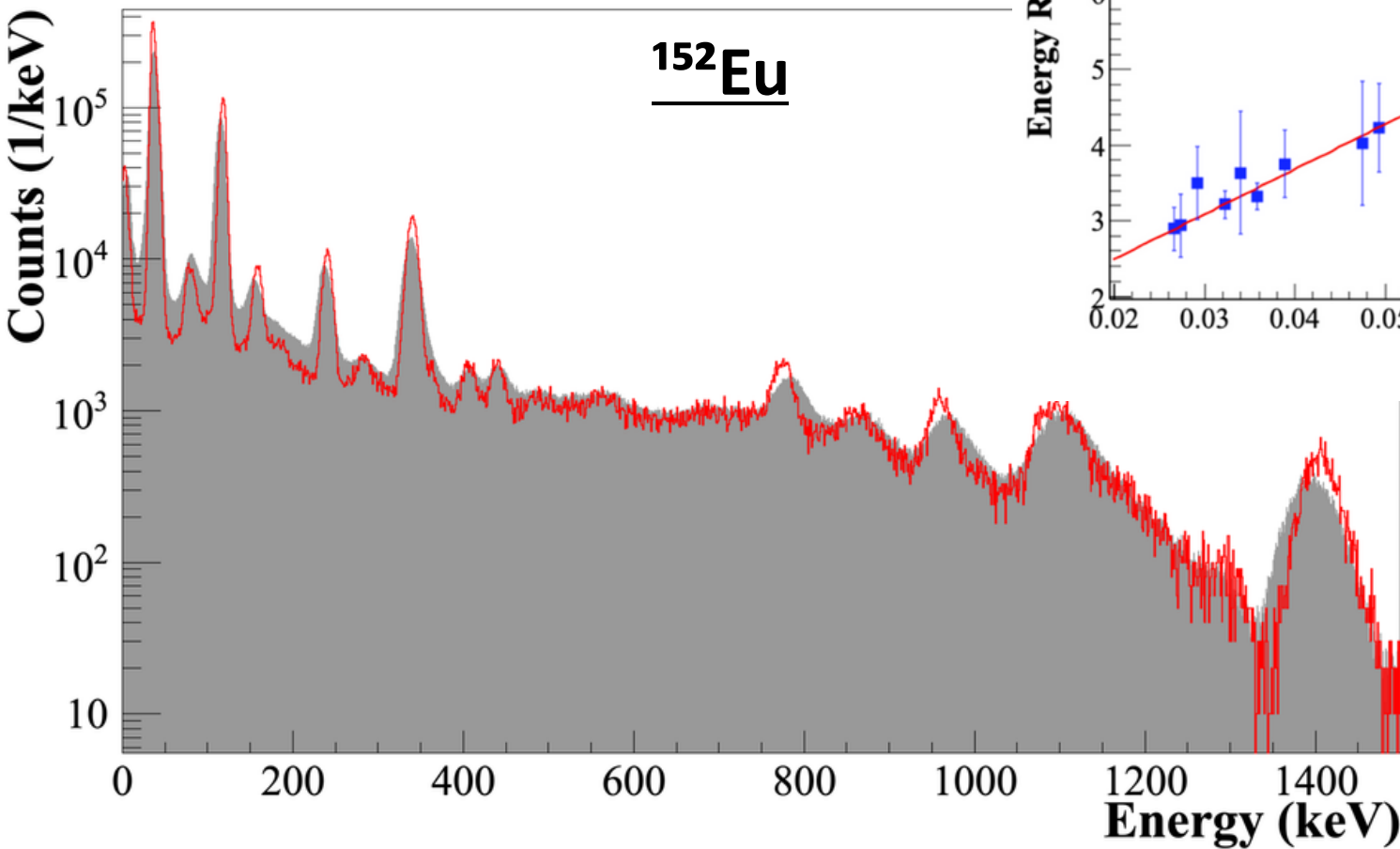
Triangular Optimisation of slow signal (Flat top = 0

$\tau = 278.02(2)$ ns

3.41(20) % @ 662 keV

Distance (mm)	344.28 keV			968.08 keV		
	$\epsilon_{EXP,FEPE}$ (%)	$\epsilon_{SIMU,FEPE}$ (%)	Agreement (σ)	$\epsilon_{EXP,FEPE}$ (%)	$\epsilon_{SIMU,FEPE}$ (%)	Agreement (σ)
10.0	1.38(19)	1.50(10)	0.56	0.223(63)	0.196(13)	0.42
30.0	0.332(142)	0.449(90)	0.70	0.123(31)	0.078(21)	1.20
50.0	0.141(16)	0.204(53)	1.14	0.042(39)	0.039(12)	0.074
100.0	0.043(7)	0.044(9)	0.088	0.009(17)	0.009(10)	0

Table Comparison of experimental and simulation for the LaBr$_3$:Ce DA absolute full-energy peak efficiencies and associated uncertainties for gamma-ray energies 344.28 keV and 968.08 keV at various source-to-detector distances.

Results of CC Simulation

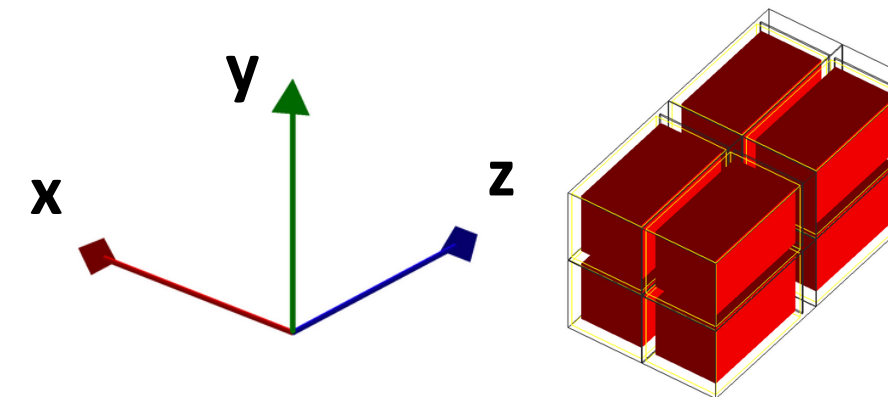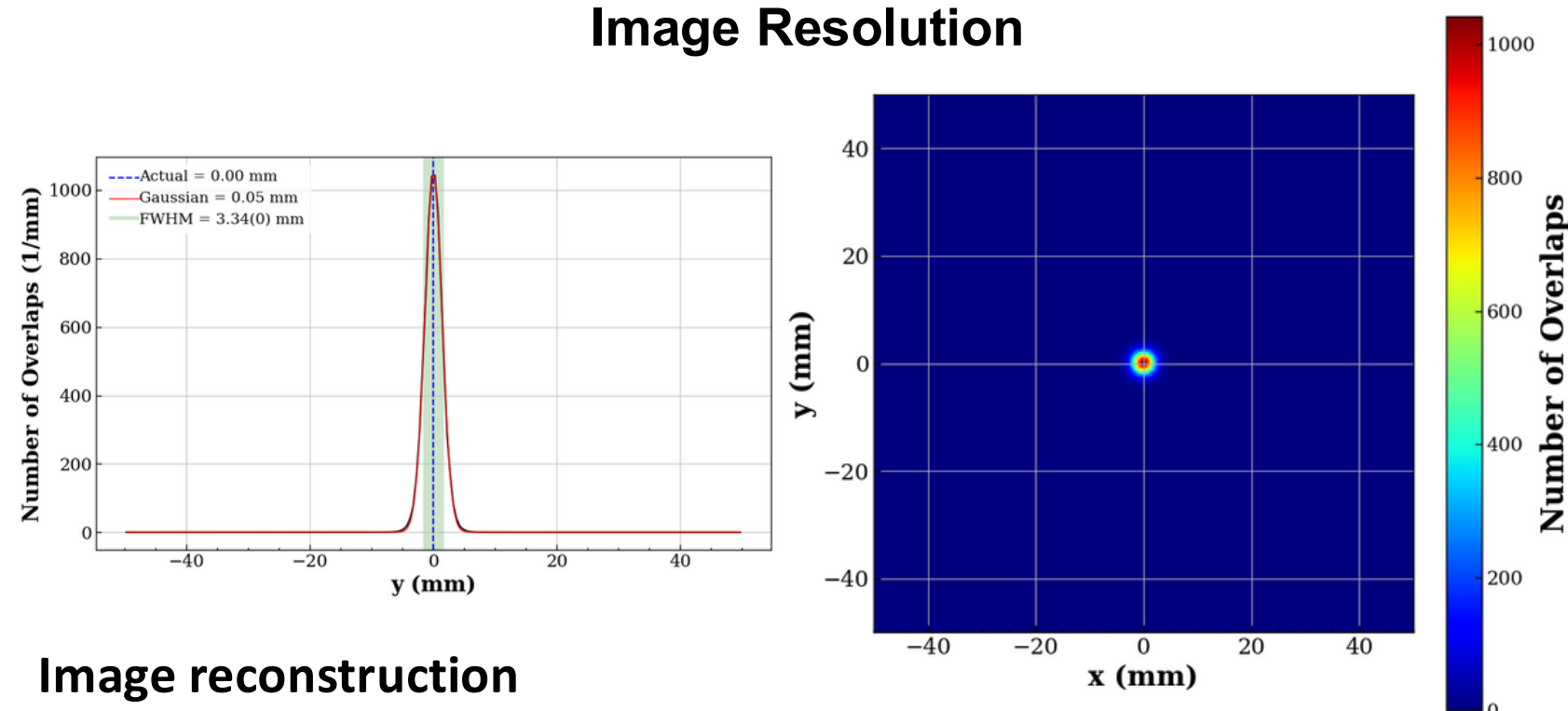**Measurements performed with ¹³⁷Cs Source at (0,0,10) mm from scatterer face**
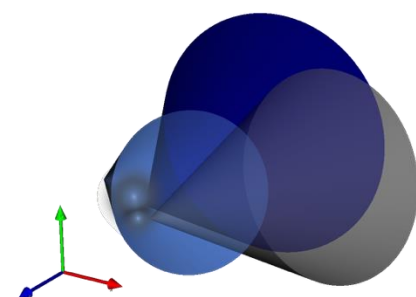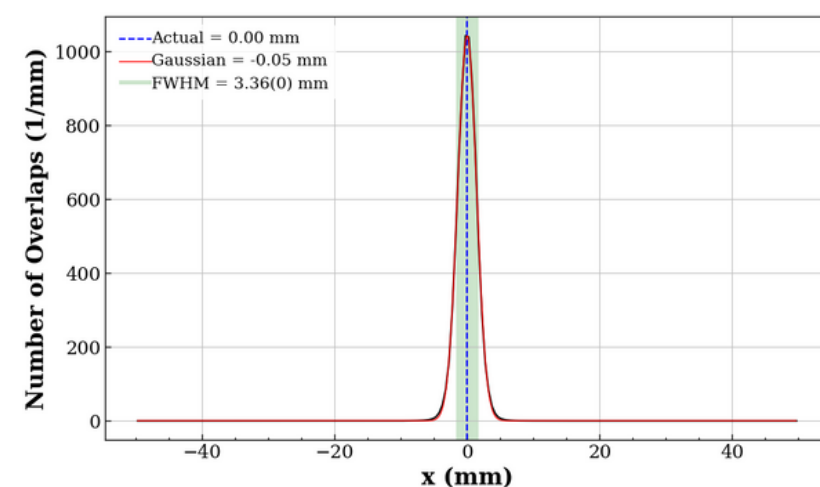

Image Resolution

Image reconstruction performed using an iterative Filtered Back Projection algorithm

- Cone A — example event path
- Cone B — example event path
- Cone C — example event path

Angular Resolution Measurement

$$ARM = \theta_{geo} - \theta_{CS}$$

$$\theta_{geo} = cos^{-1}\left(\frac{(r_S - r_0)\cdot(r_A - r_S)}{|r_S - r_0|\cdot|r_A - r_S|}\right)$$

$$\theta_{CS} = cos^{-1}\left(1 - m_e c^2\left(\frac{1}{E_A} - \frac{1}{E_S + E_A}\right)\right)$$

$$m_e c^2 = 510.9989461 \text{ keV}$$
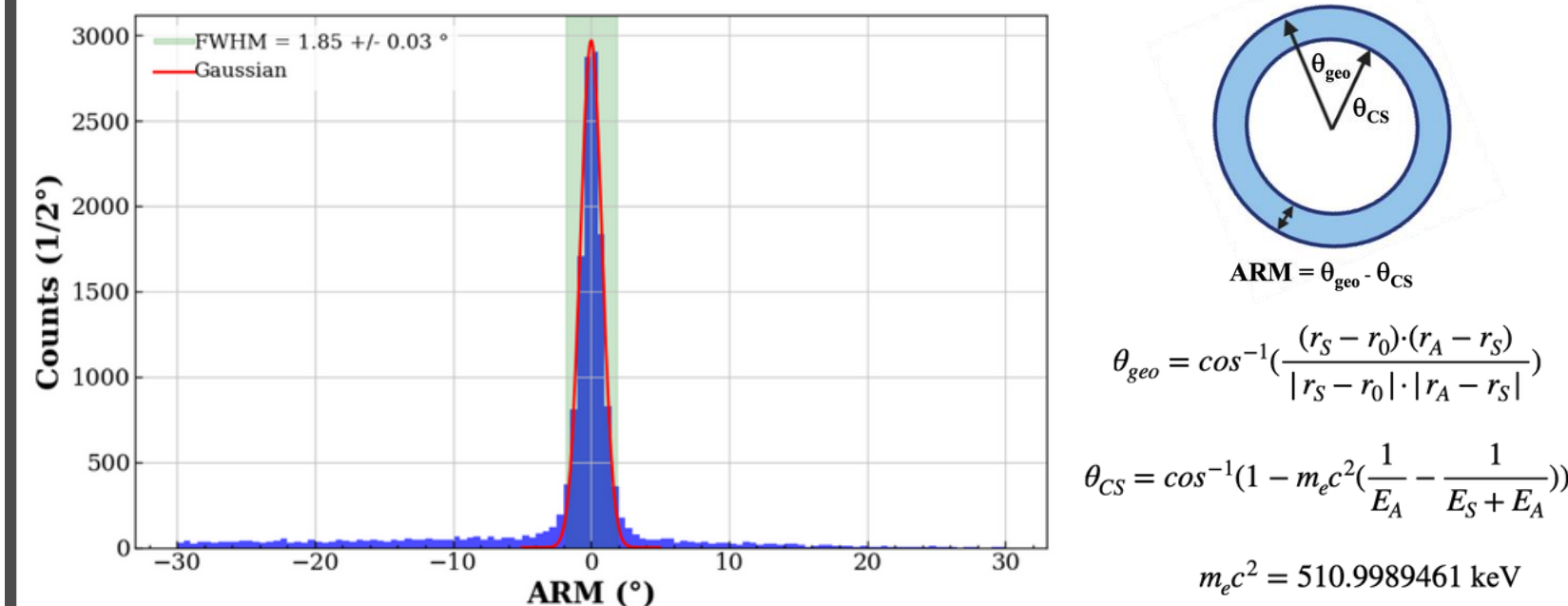
The Effect of CC Backscattering
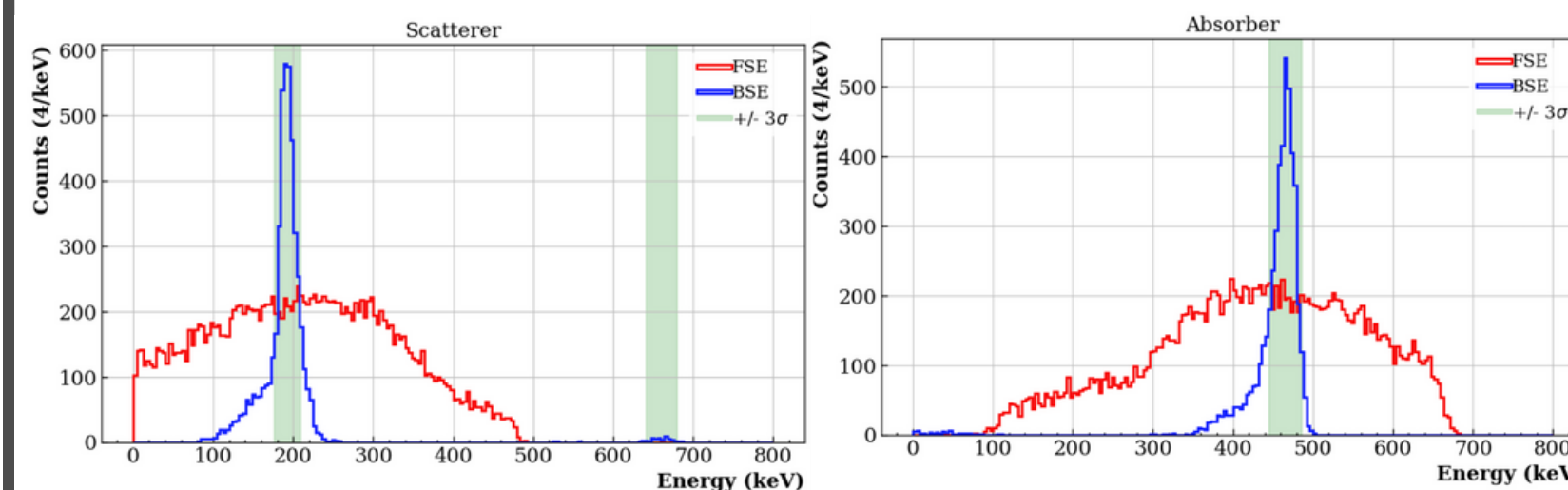
DA Fast Timing Performance

Calculated by gating on the ^{60}Co prompt-gamma decays. The time interval between the **1173 keV** and **1332 keV** emissions is **<0.9 ps**, effectively instantaneous compared to detector resolution.
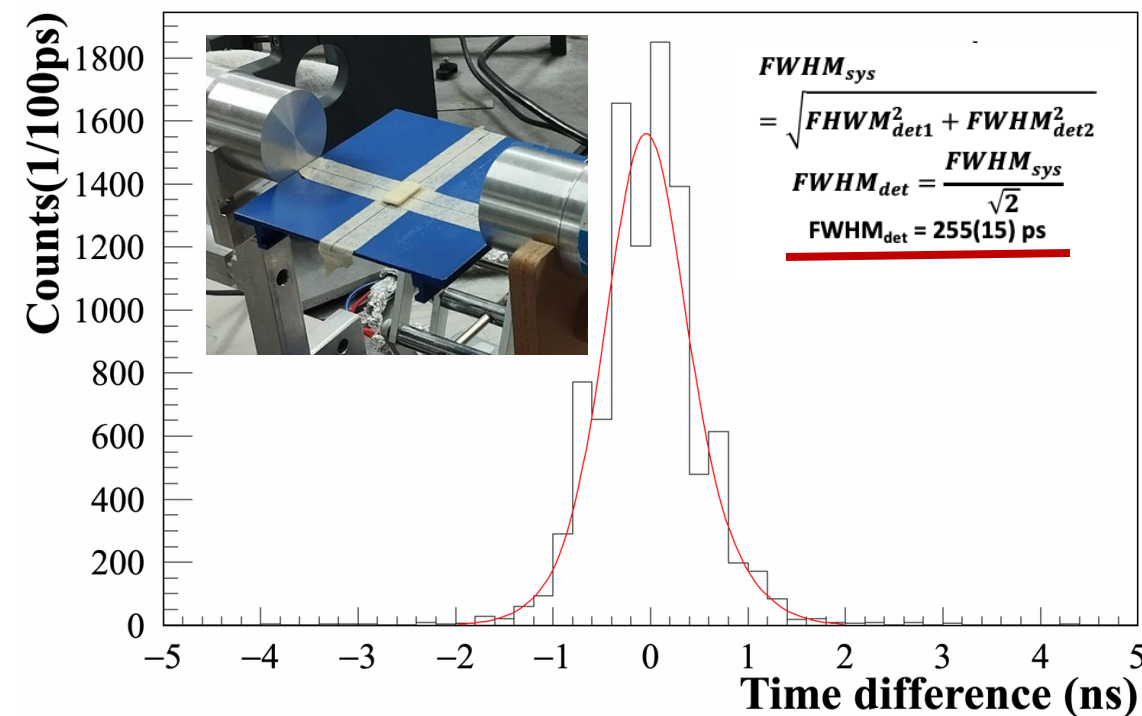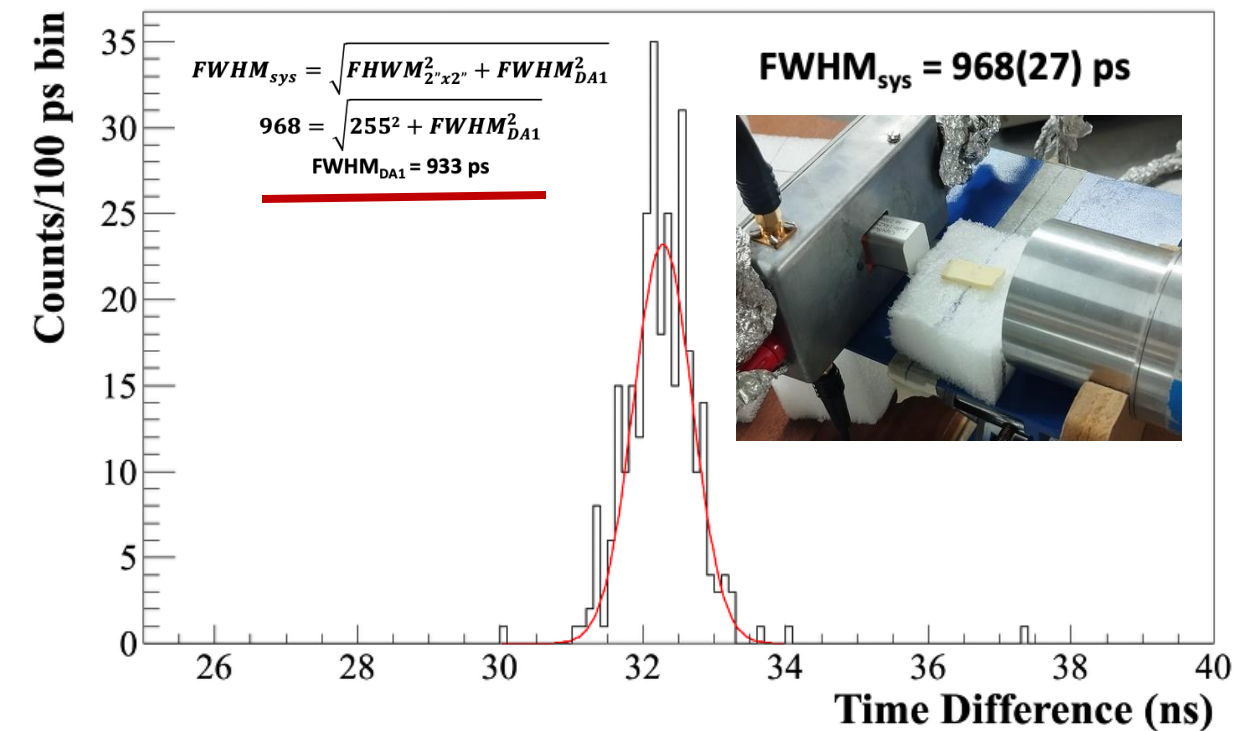
Measurements performed using the **14-bit XIA PIXIE-16 500 MHz** data acquisition system, exploiting the use of the **digital CFD** for fast timing.
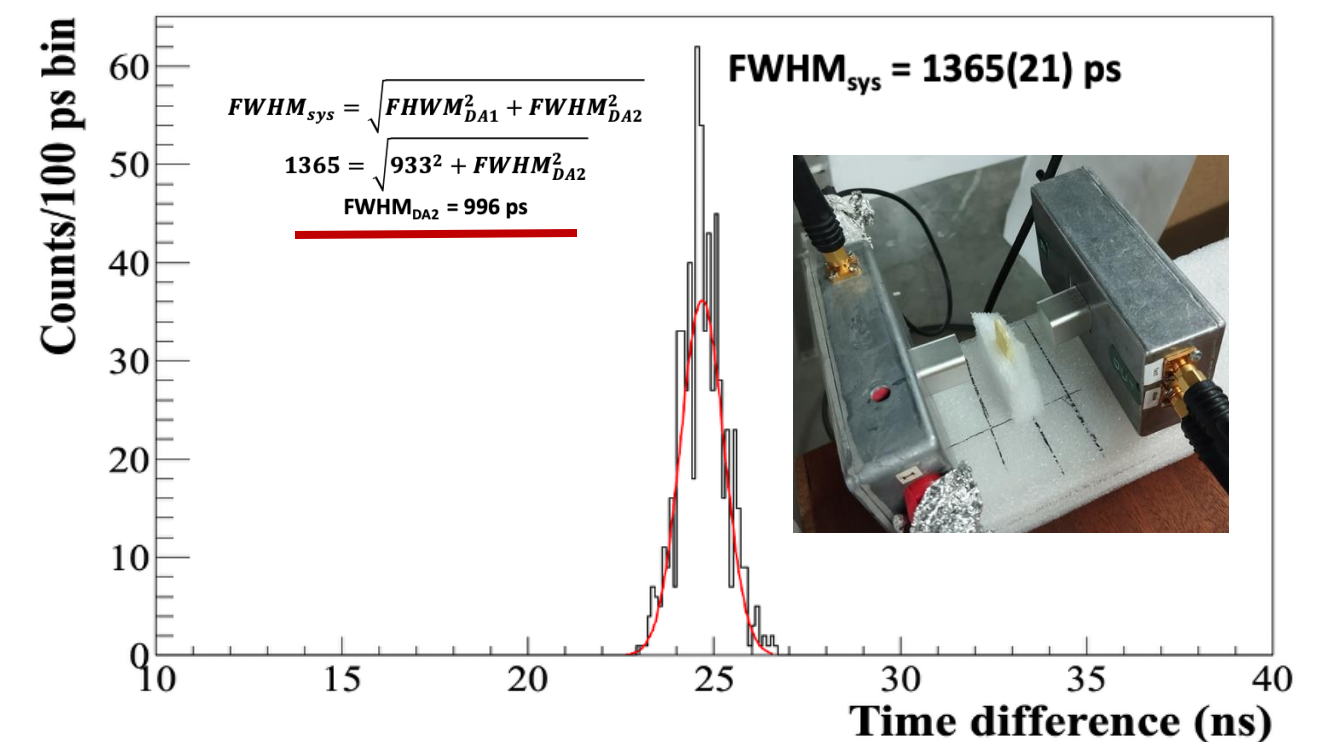
Two 2" x 2" LaBr$_3$:Ce detectors

$$FWHM_{sys} = \sqrt{FHWM_{det1}^2 + FWHM_{det2}^2}$$
$$FWHM_{det} = \frac{FWHM_{sys}}{\sqrt{2}}$$
$$FWHM_{det} = 255(15) \text{ ps}$$

2" x 2" and DA LaBr$_3$:Ce detectors

$$FWHM_{sys} = \sqrt{FHWM_{2"x2"}^2 + FWHM_{DA1}^2}$$
$$968 = \sqrt{255^2 + FWHM_{DA1}^2}$$
$$FWHM_{DA1} = 933 \text{ ps}$$

$$FWHM_{sys} = 968(27) \text{ ps}$$

Two LaBr$_3$:Ce DAs

$$FWHM_{sys} = \sqrt{FHWM_{DA1}^2 + FWHM_{DA2}^2}$$
$$1365 = \sqrt{933^2 + FWHM_{DA2}^2}$$
$$FWHM_{DA2} = 996 \text{ ps}$$

$$FWHM_{sys} = 1365(21) \text{ ps}$$

Postdoctoral Research

Current & Upcoming Work

Position-sensitive detection in LaBr$_3$:Ce scintillators
Improving spatial resolution using **Broadcom AFBR-S4N44P164M 4×4 SiPM arrays**
Custom development boards currently in production
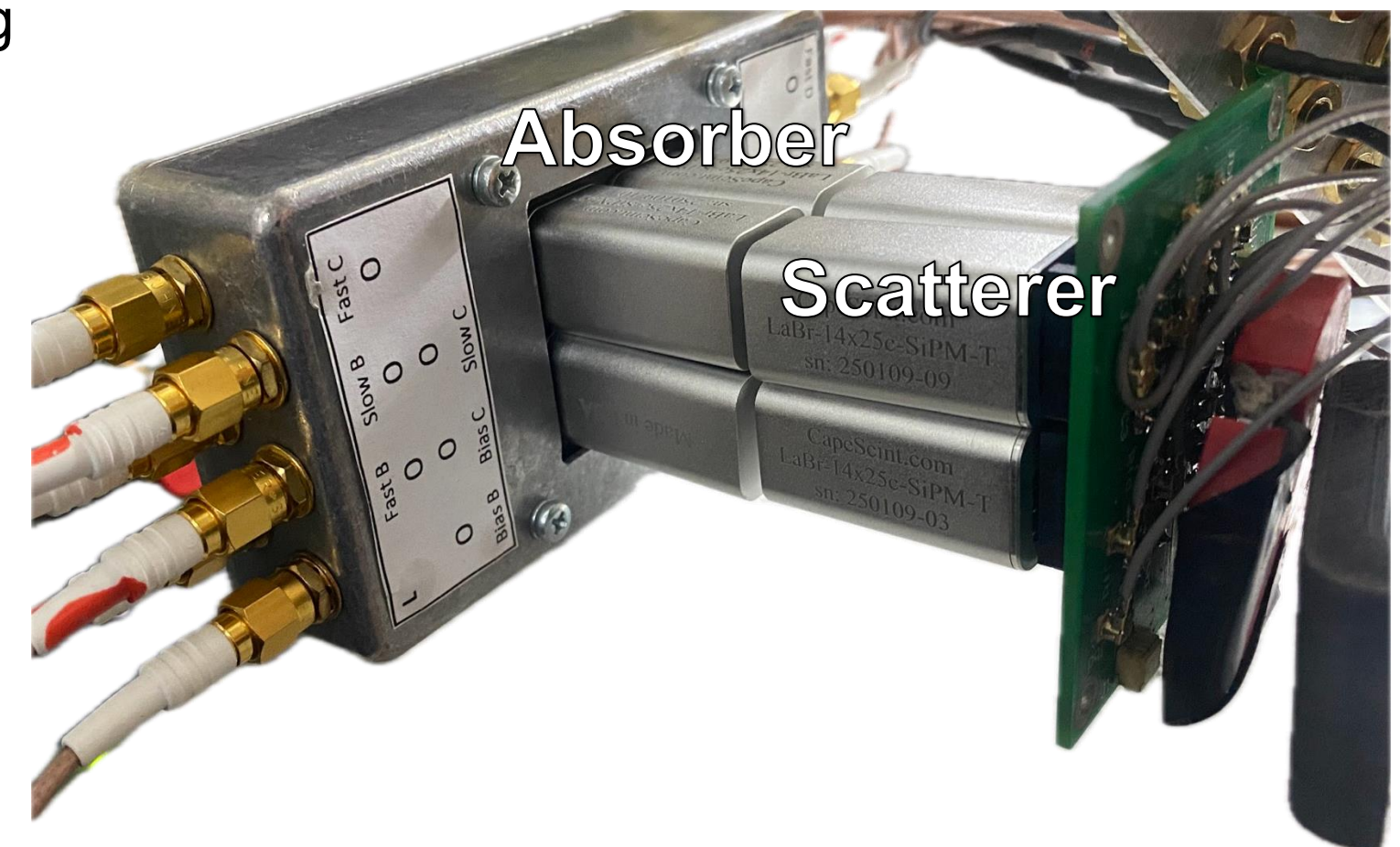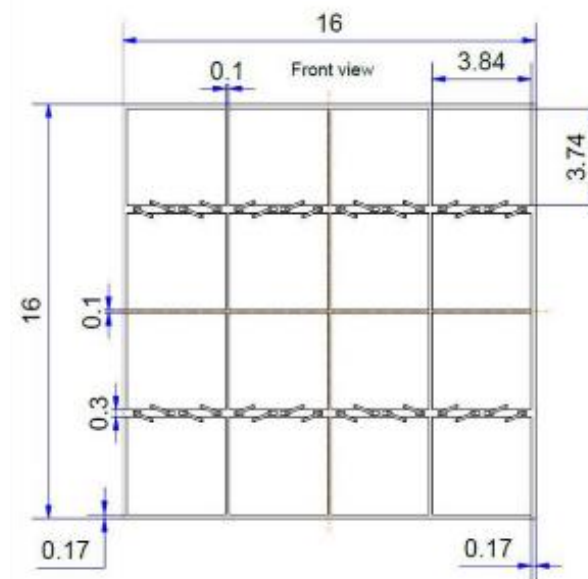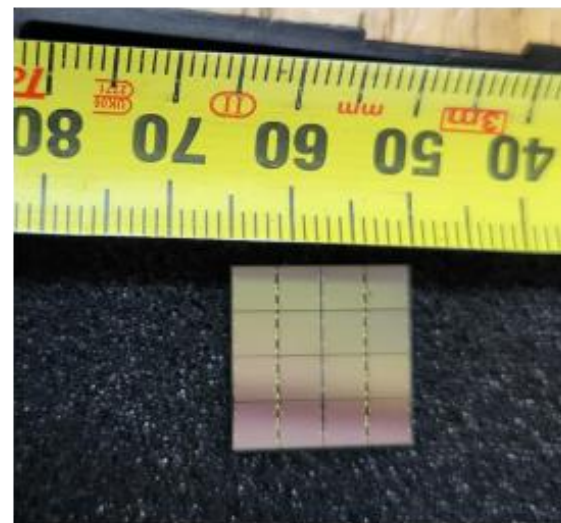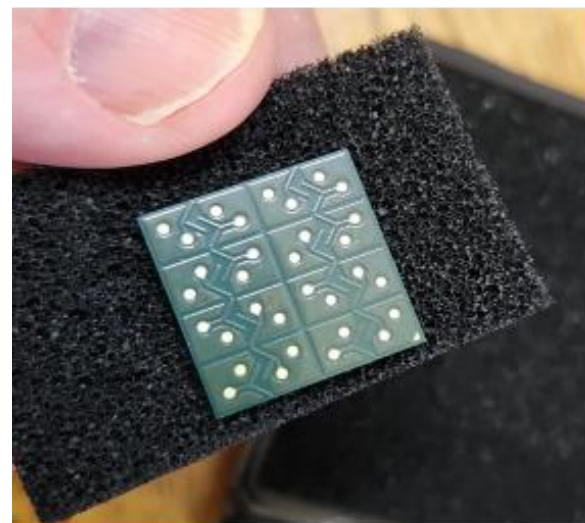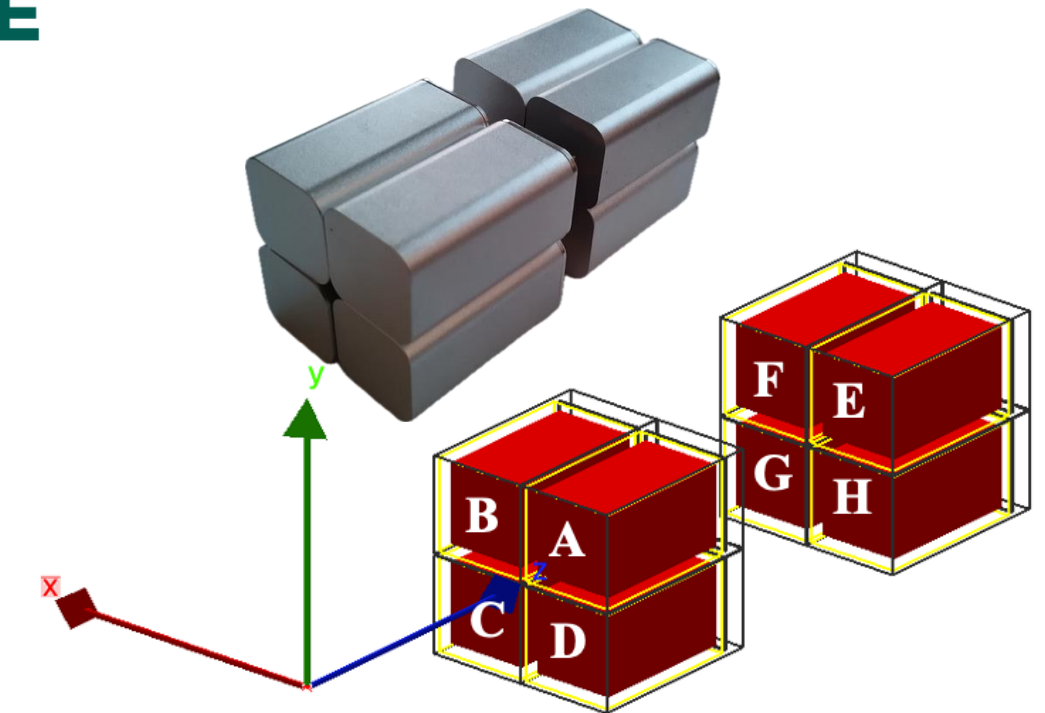**Enhanced Geant4 simulations**
Realistic performance modelling for detector optimisation
Drone-based deployment of Compton Cameras
Environmental monitoring and mapping applications
In-beam proton testing
Evaluation with **70 MeV and 200 MeV proton beams** for medical imaging

PANGoLINS Project

The **P**ortable **A**frican **N**eutron-**G**amma **L**aboratory for **I**nnovative **N**uclear **S**cience

Milestones

Reduce footprint of the Mobile Radiation Detection Unit

Adopt next-generation detectors

→ $LaBr_3$, SrI_2, CLYC (Cs_2LiYCl_6)

Enable neutron sensitivity

→ Effective gamma–neutron discrimination

Transition from photomultipliers to SiPMs

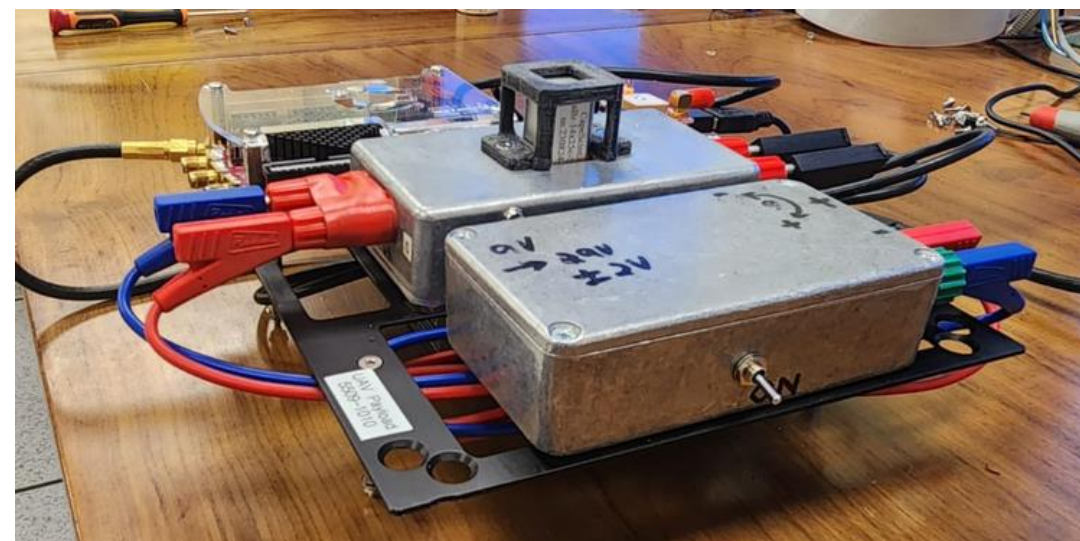→ Compact, low-power silicon avalanche photodiodes

Eliminate high-voltage requirements

→ Move to stable low-voltage operation

Characterise and deploy advanced measurement systems

Expand field testing

→ On-foot surveys and drone-based in-situ deployments

CLYC-6 for Thermal Neutron Detection

Measurements:
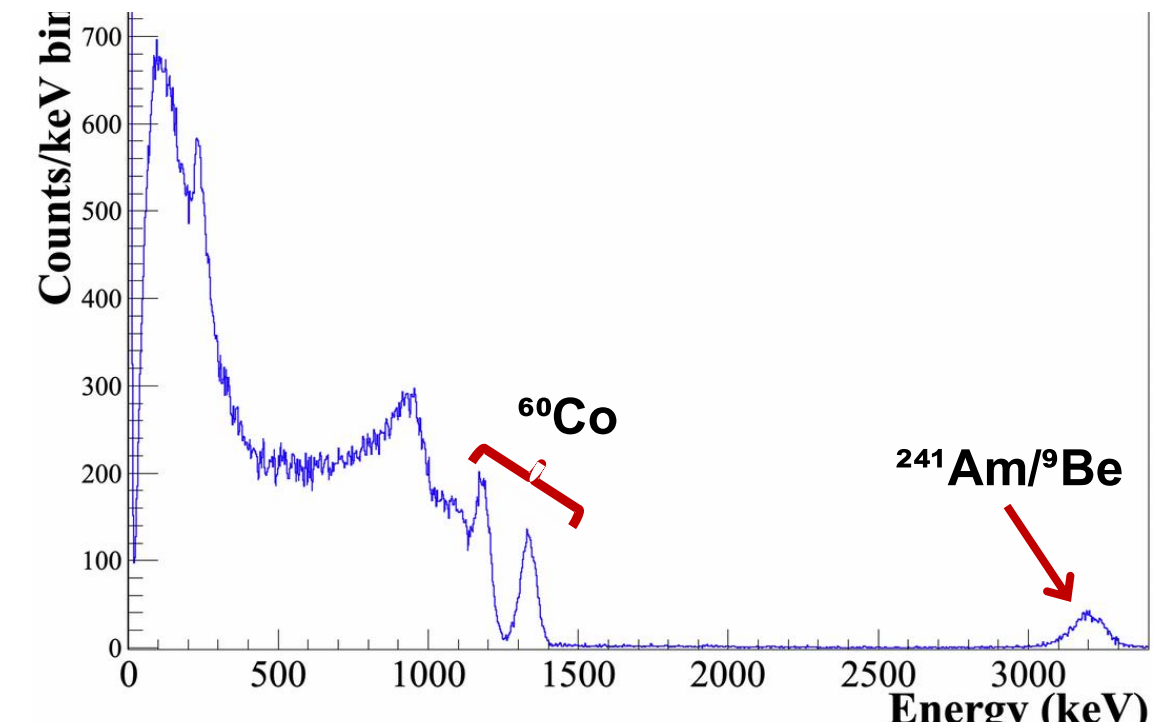$^{241}Am/^9Be$ **neutron source** (6.9 GBq) and ^{60}Co **gamma source**
PIXIE-16 500 MHz DAQ
Elpasolite crystal Cs_2LiYCl_6:Ce (^6Li = 95%) detector **slow signal**.

$^6Li+n\rightarrow^3H$(2.73 MeV)+α(2.05 MeV) Q-value = 4.78 MeV, σ = 940 barns at
En = 0.025 eV.
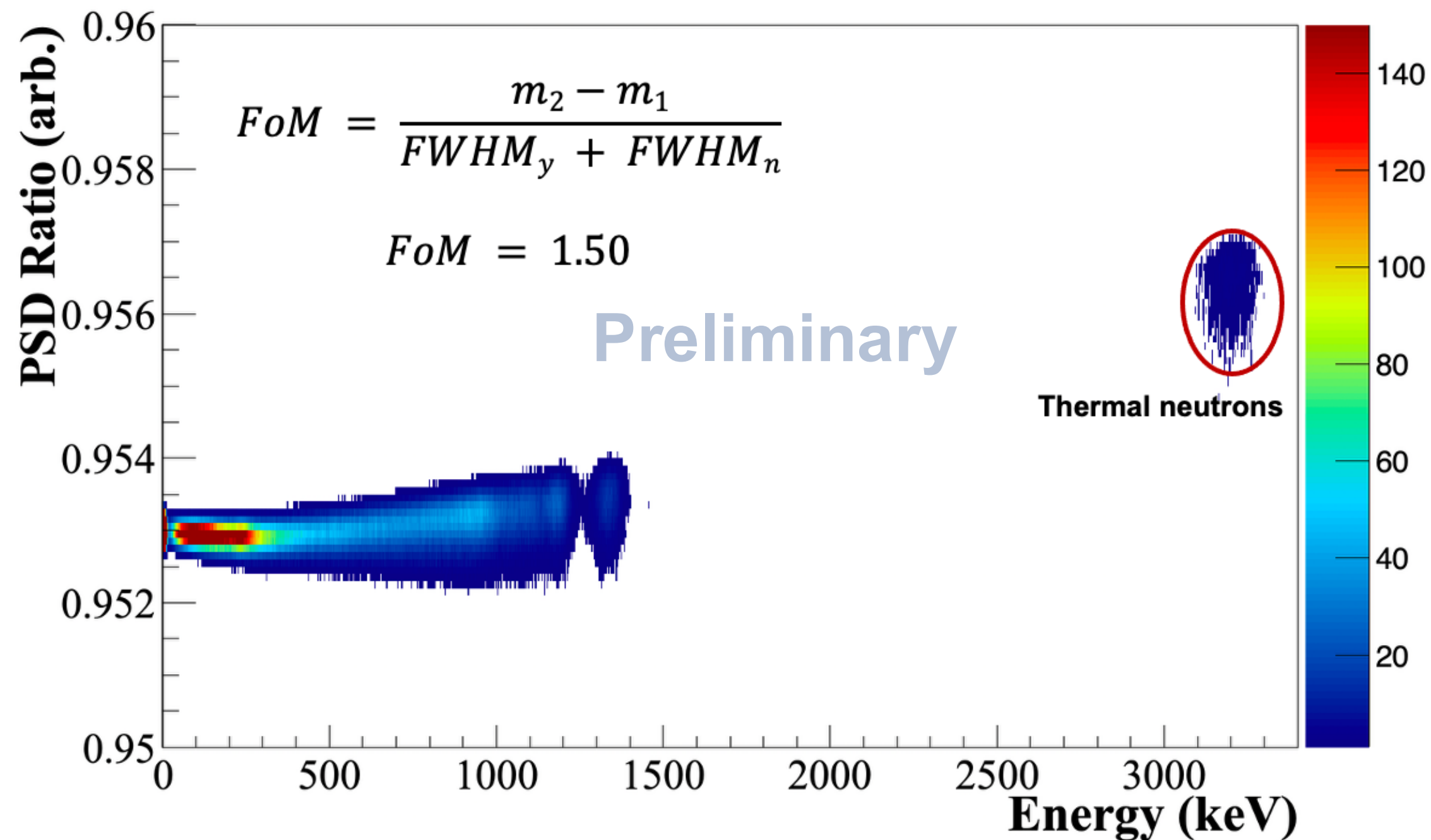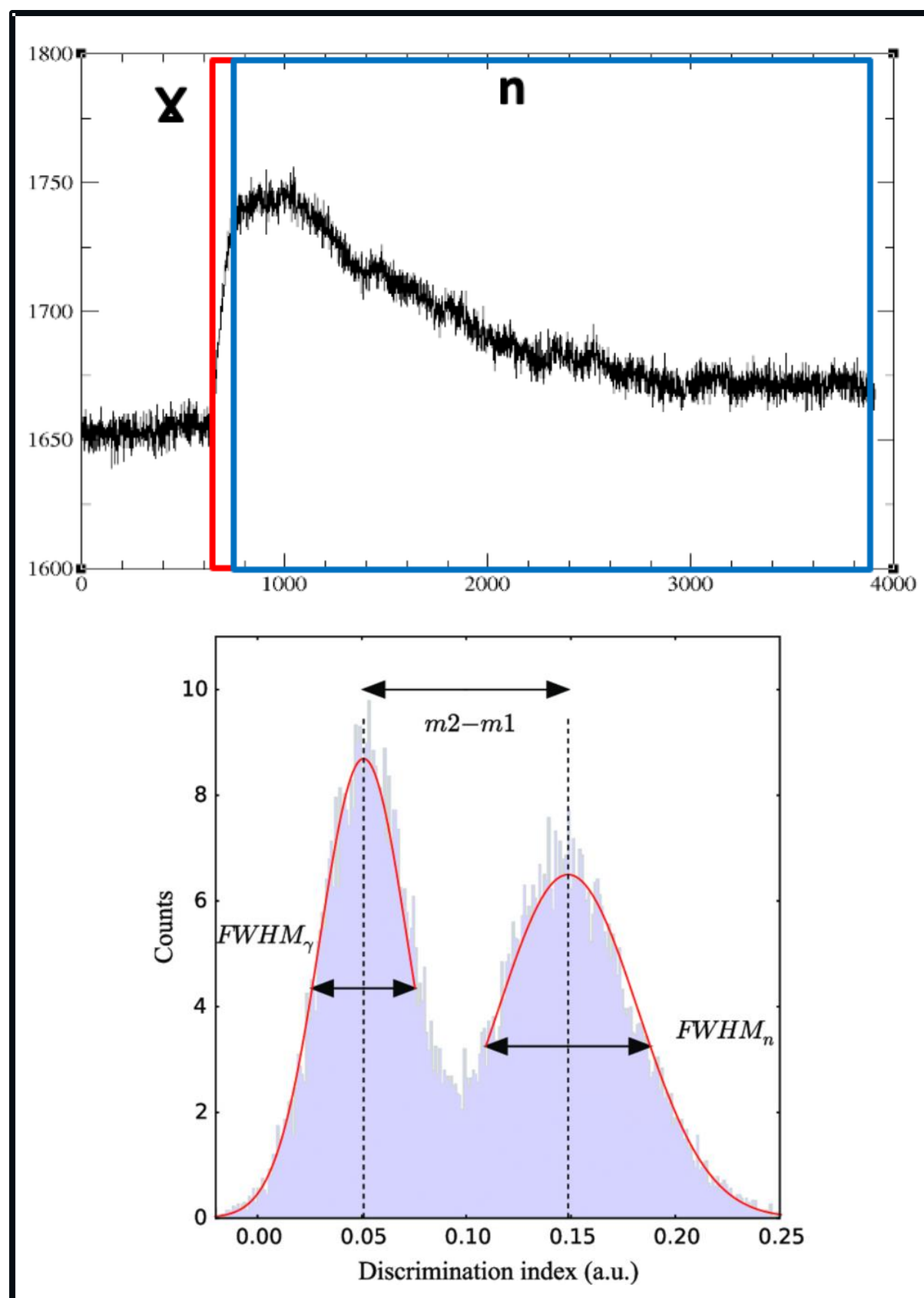$^{35}Cl+n\rightarrow^{35}S+p$

3.2 MeV thermal neutron peak observed due to quenching effects.

PSD is based on the difference in the scintillation decay response to gamma and neutrons

Signal Rise Times

QCD Sums Trace Capture

CLYC Traces

$$FoM = \frac{m_2 - m_1}{FWHM_\gamma + FWHM_n}$$

$$FoM = 1.50$$

Preliminary

Thermal neutrons

Advancing knowledge. Transforming lives. Inspiring a nation.

DASSIE Project

Digital Acquisition Signal System for Innovative Experimentation

Goal: Develop a **low-power**, **low-cost**, **lightweight**, and **scalable** streaming digitiser for real-time radiation detection.

Applications: Medical imaging, environmental monitoring, and security.

Key Features:
- Local **pulse shape analysis**, real-time **network streaming**, and time-stamped data storage.
- Compatible with **small-volume scintillator detectors**
- **Wireless user interface** for control and data access.

Hardware Specs:
Digitisation: 1 GHz, 14-bit ADC, ±1 V range

Firmware Features:
- Digital Leading-Edge / CFD
- Moving Window Deconvolution (adaptive preferred)
- Pile-up detection
- 8 user-defined integration windows
- External trigger handling to reduce data rate

A d v a n c i n g   k n o w l e d g e.   T r a n s f o r m i n g   l i v e s.   I n s p i r i n g   a   n a t i o n.

S. Hart – ANPC 2025

Acknowledgements

Collaborators & Contributors

Dr. Pete Jones

Assoc. Prof. Luna Pellegri

Prof. Steve Peterson

Mr. Christo van Tubergh

Dr. Philippos Papadakis

Mr. Moschos Kogimtzis

Dr. Carl Unsworth

Dr. Matthew Russell

Dr. Marc Labiche

Advancing knowledge. Transforming lives. Inspiring a nation.

Thank you for your attention

My email address: shanynhart@tlabs.ac.za

Questions?

Back-up slides
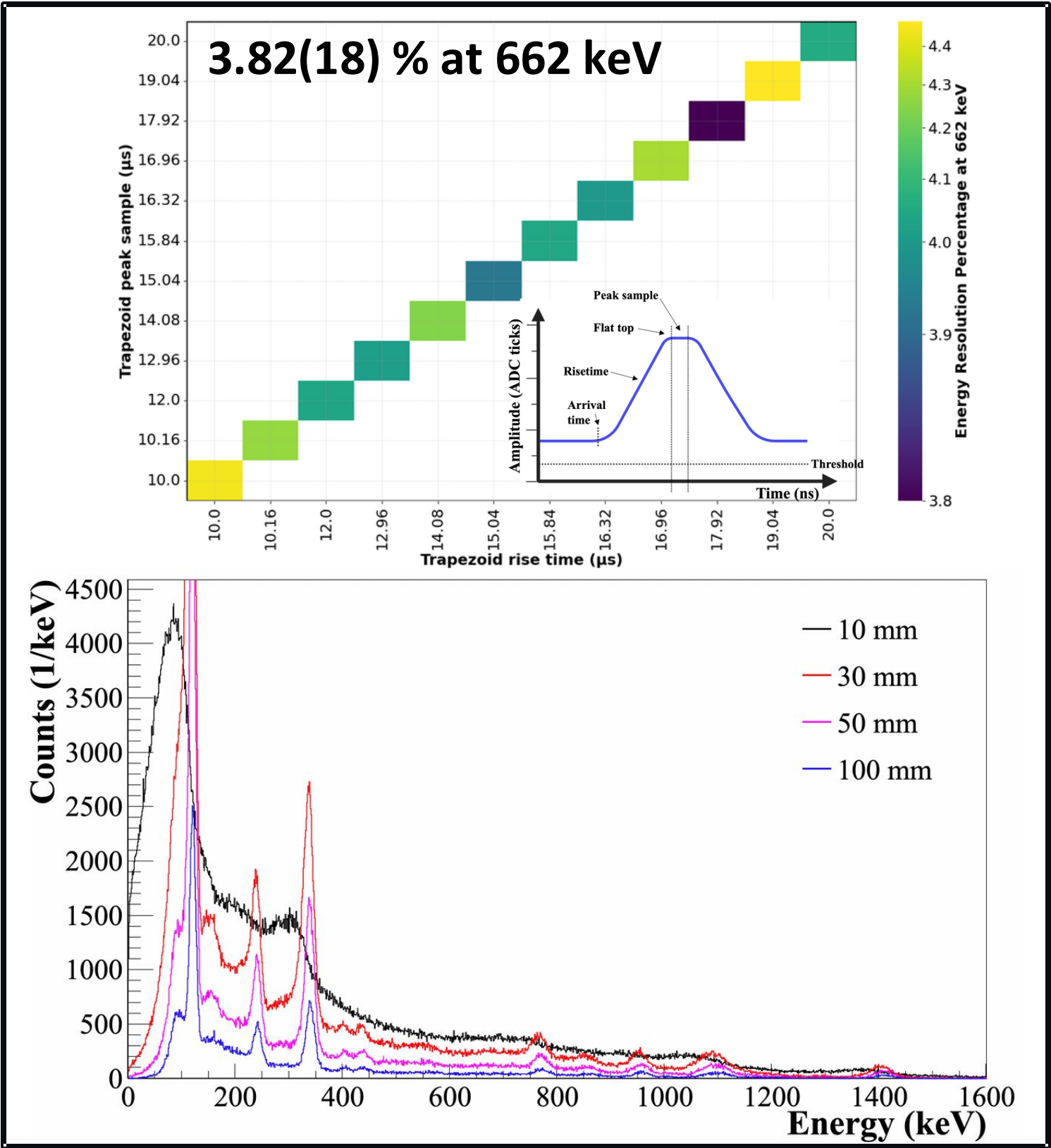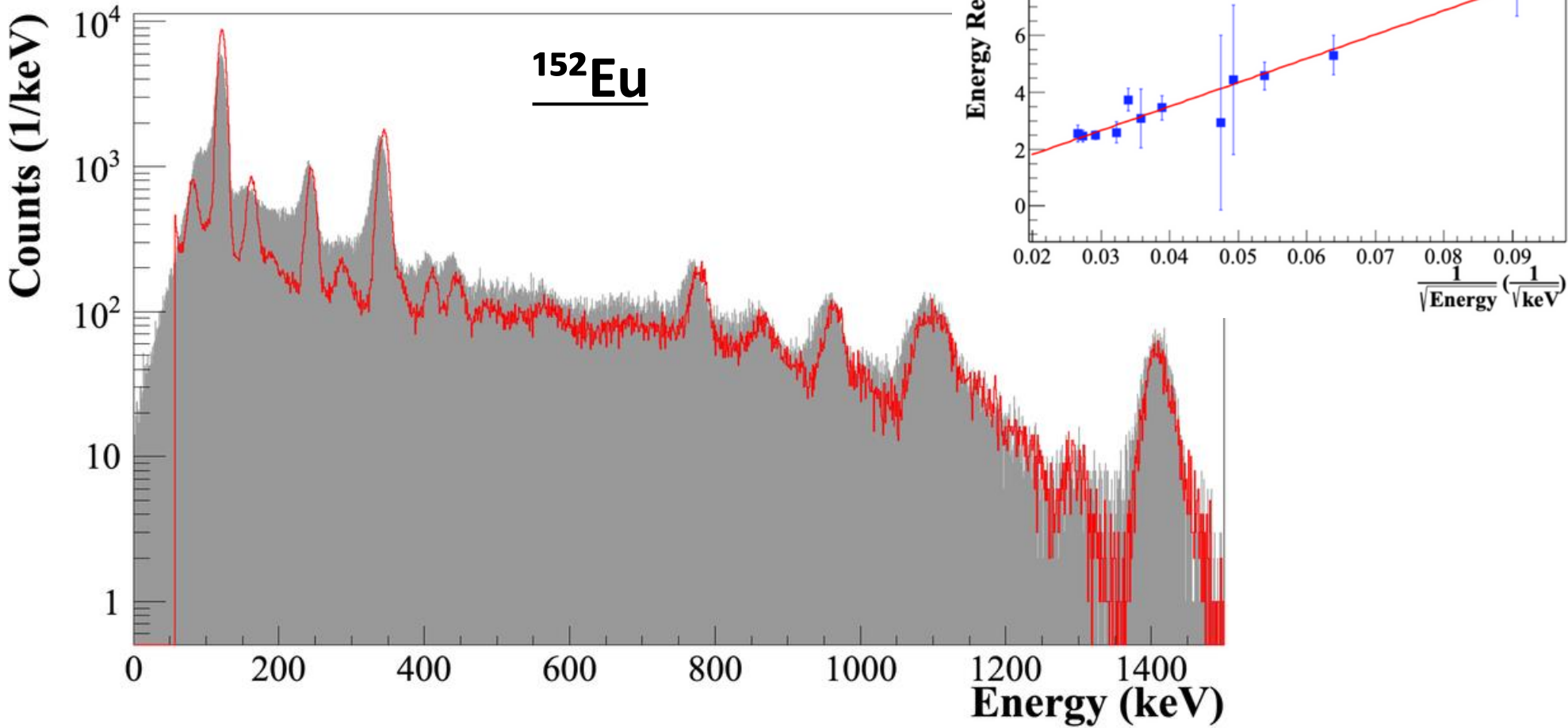
Advancing knowledge. Transforming lives. Inspiring a nation.

SrI$_2$:Eu-SiPM

^{152}Eu

$$R(E) = \frac{84.25(1263)}{\sqrt{E}} + 0.13(41)$$

$\chi^2/\text{NDF} = 0.55$

3.82(18) % at 662 keV

Distance (mm)	344.28 keV			968.08 keV		
	$\epsilon_{EXP,FEPE}$ (%)	$\epsilon_{SIMU,FEPE}$ (%)	Agreement (σ)	$\epsilon_{EXP,FEPE}$ (%)	$\epsilon_{SIMU,FEPE}$ (%)	Agreement (σ)
30.0	0.282(87)	0.480(11)	2.26	0.053(10)	0.043(6)	0.86
50.0	0.124(15)	0.196(9)	4.12	0.031(15)	0.019(3)	0.79
100.0	0.045(6)	0.060(34)	0.43	0.011(3)	0.010(5)	0.17

Table 2 : Comparison of experimental and simulation for the SrI$_2$:Eu DA absolute full-energy peak efficiencies and associated uncertainties for gamma-ray energies 344.28 keV and 968.08 keV at various source-to-detector distances.
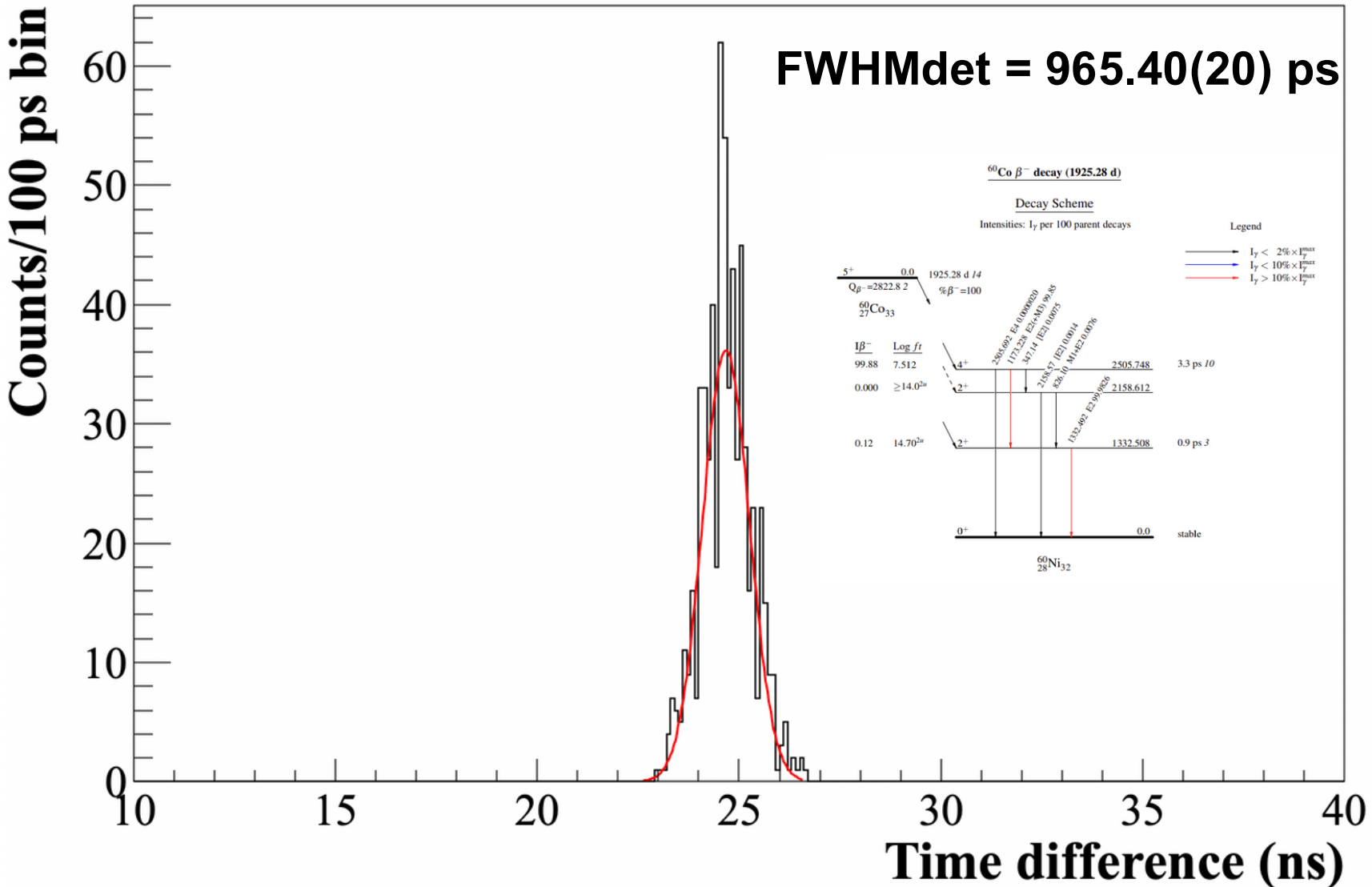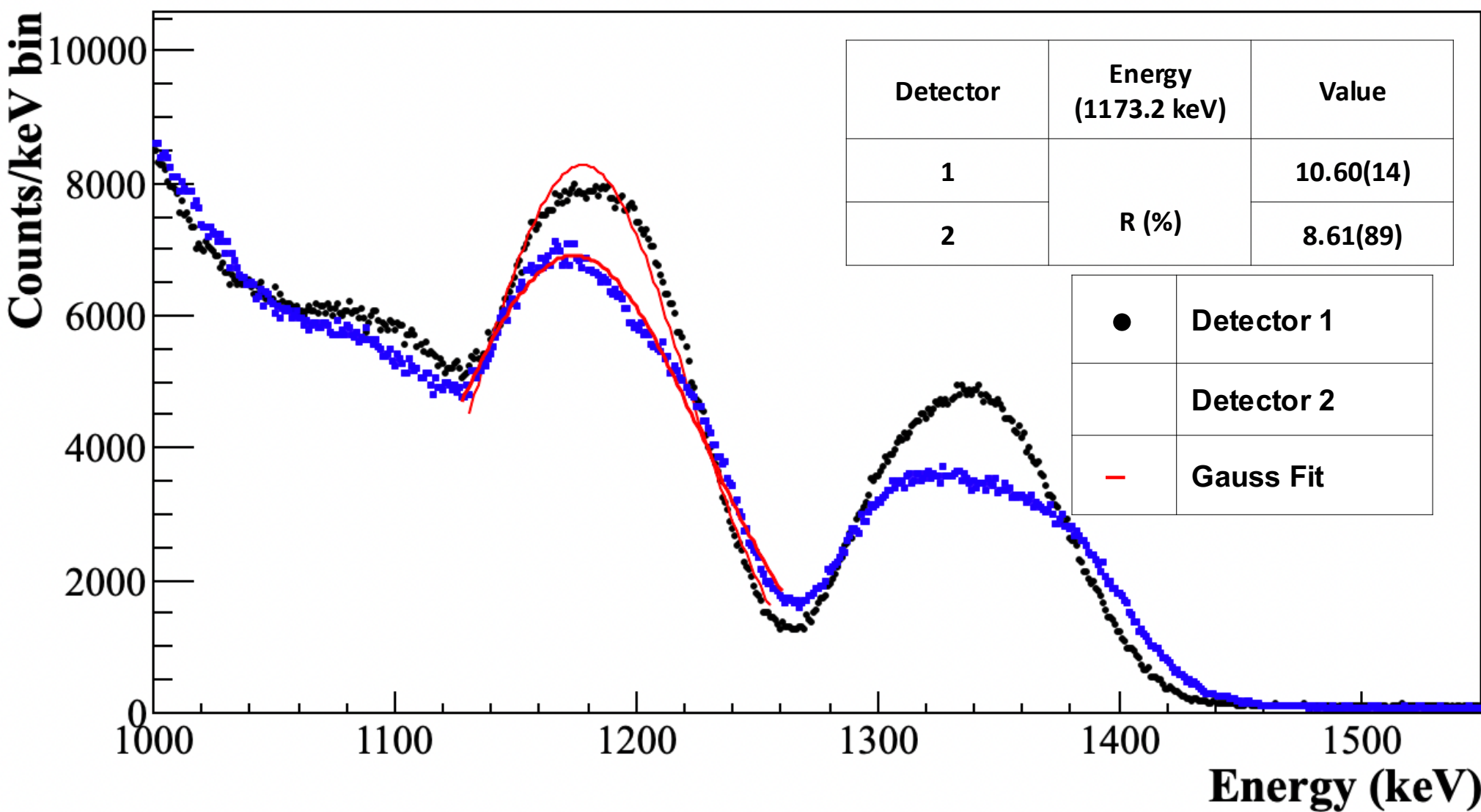
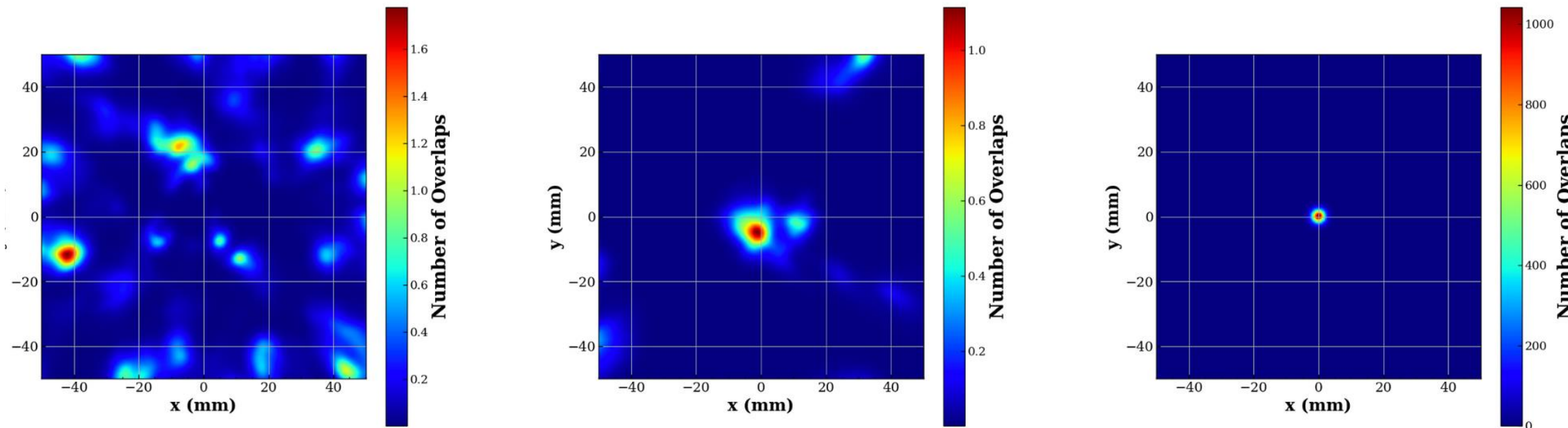Poor agreement, saturation at high count rates

SrI₂:Eu Detector Fast-Timing Resolution

Calculated by gating on the ^{60}Co prompt-gamma decays.
The time interval between the 1173 keV and 1332 keV emissions is **<0.9 ps**, effectively instantaneous compared to detector resolution.

Measurements performed using the **PIXIE-16 500 MHz** data acquisition system, exploiting the use of the **digital CFD** for fast timing.
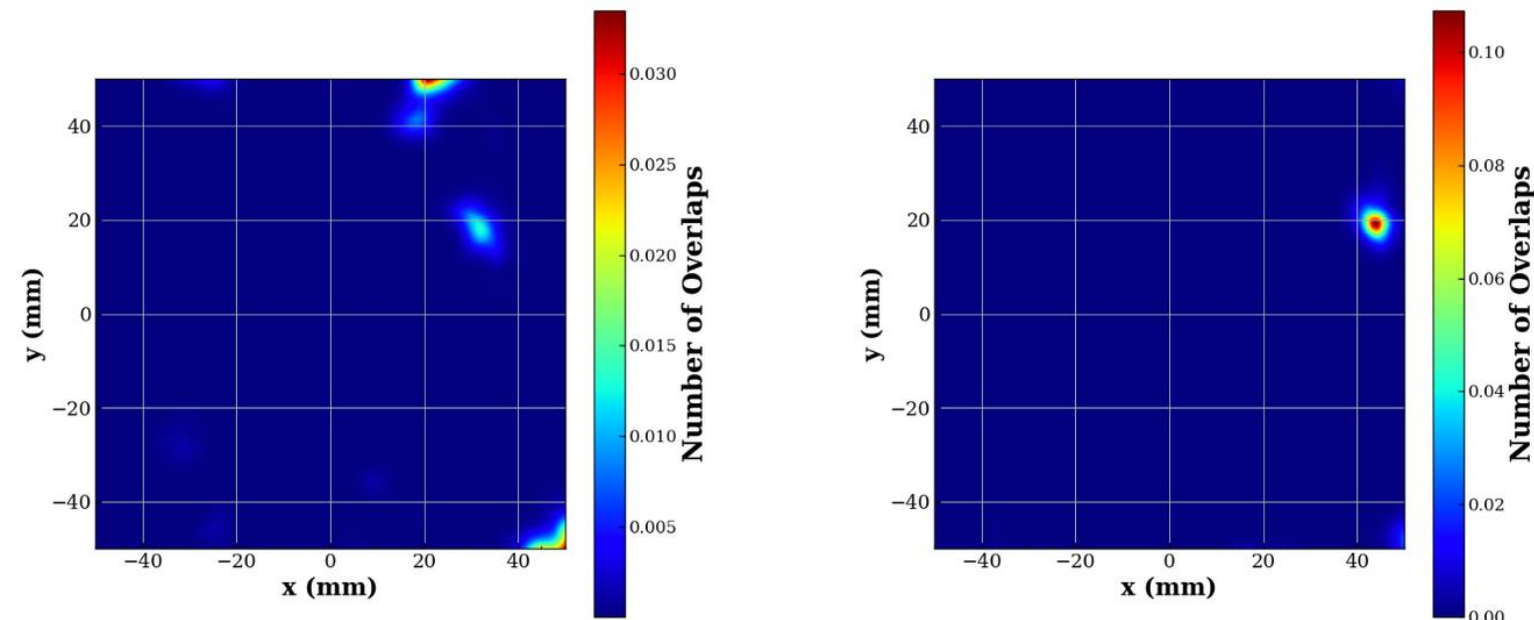

Detector	Energy (1173.2 keV)	Value
1		10.60(14)
2	R (%)	8.61(89)

- **●** Detector 1
- **■** Detector 2
- **—** Gauss Fit

FWHMdet = 965.40(20) ps

Image Reconstruction Optimisation
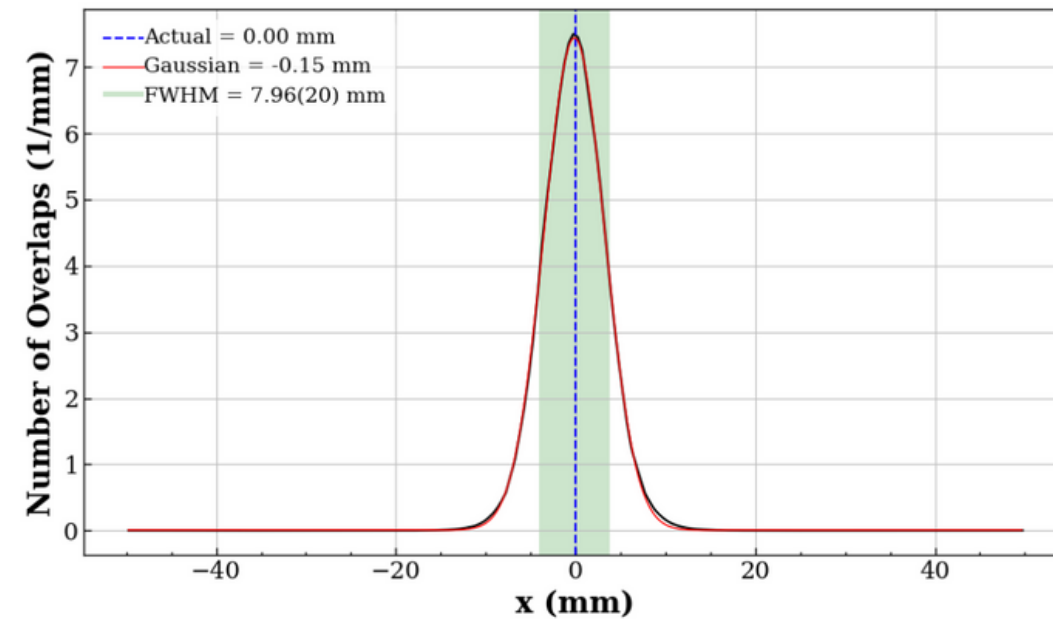

(a)

(b)

(c)

The x-y matrix of CC1 shown at different z slice values for the same Octane EM reconstruction

Image Reconstruction Optimisation

The x and y projections (sliced at the maximum y-z and x-z values respectively) of CC1 shown for different bin width in the Octane EM reconstruction.
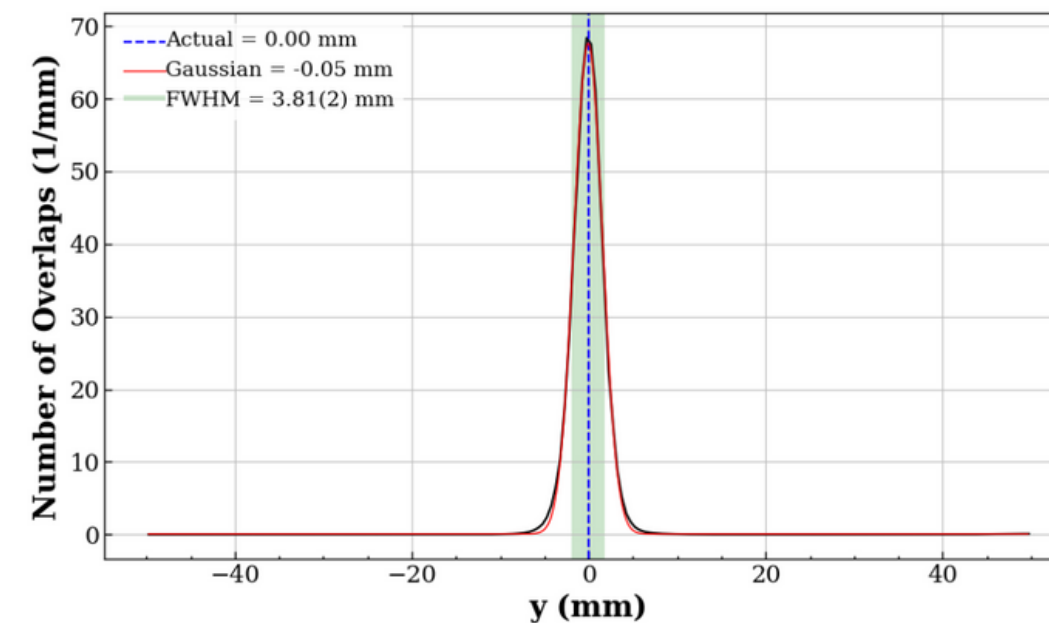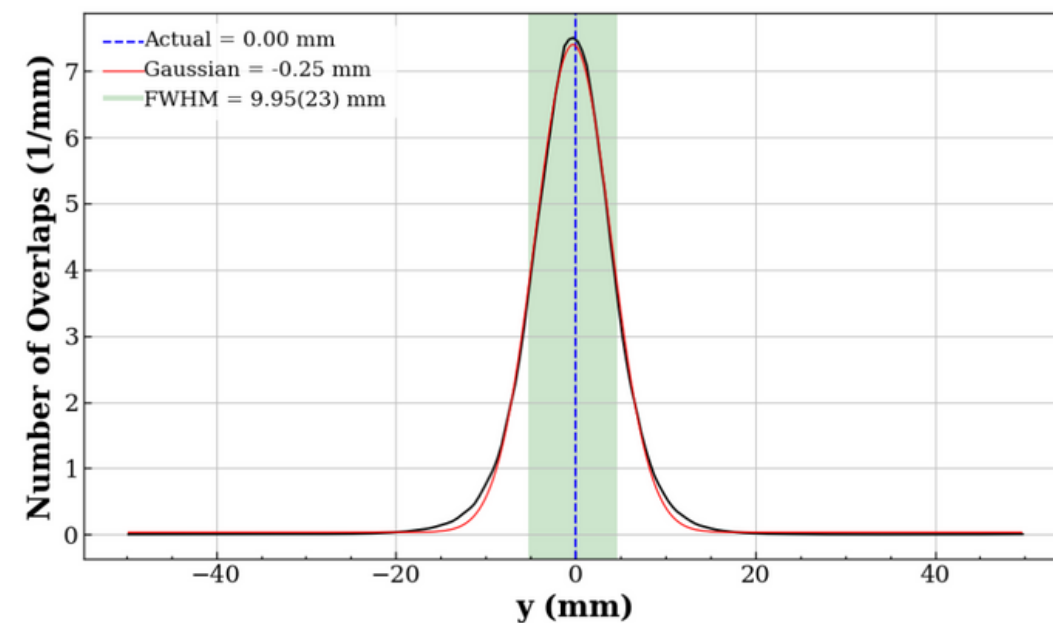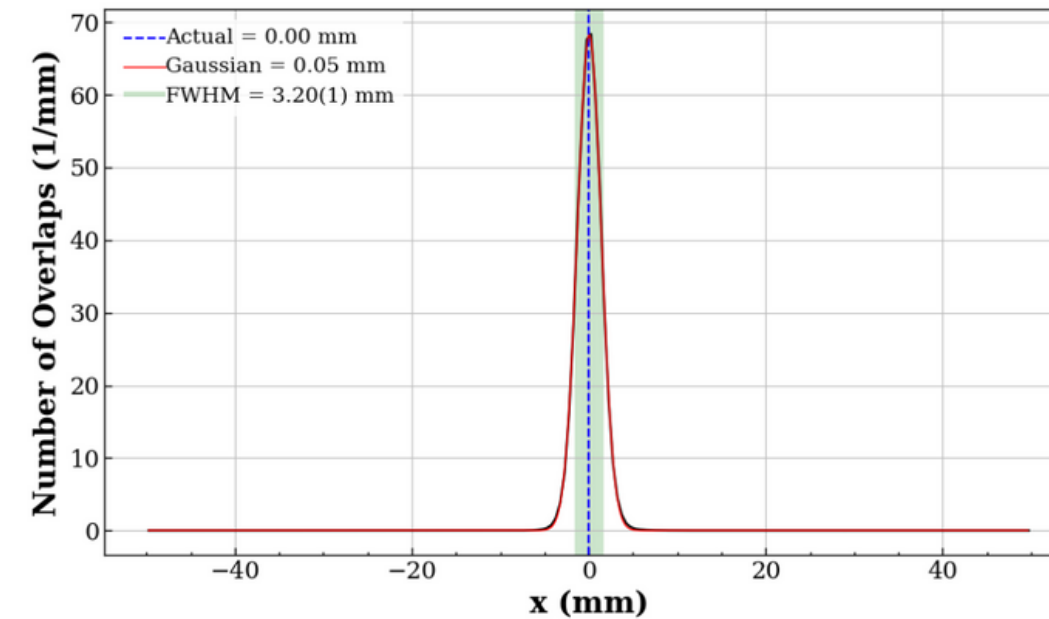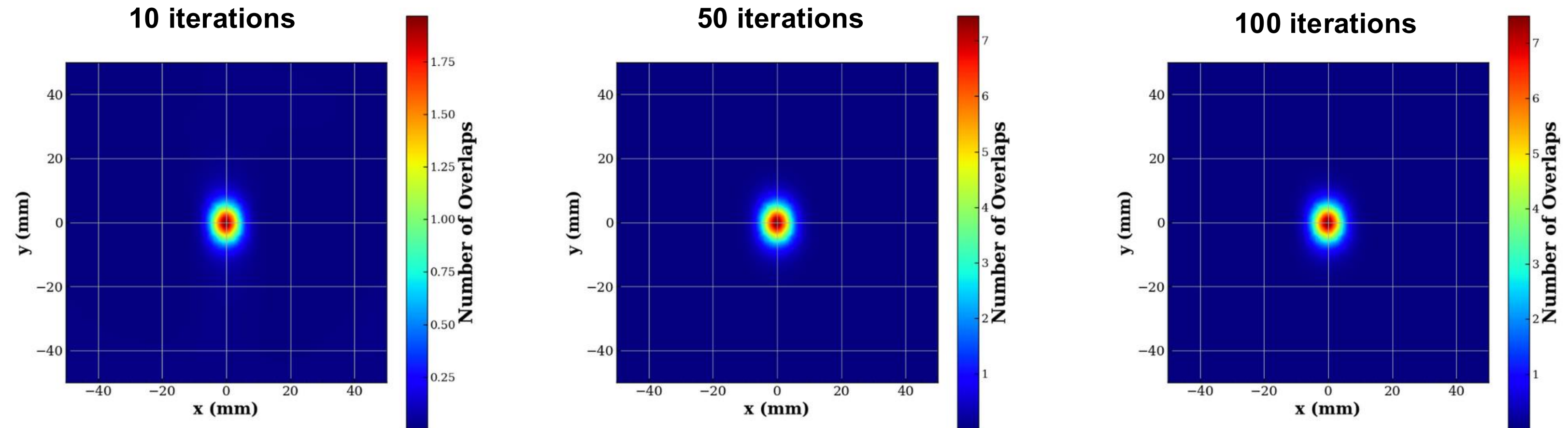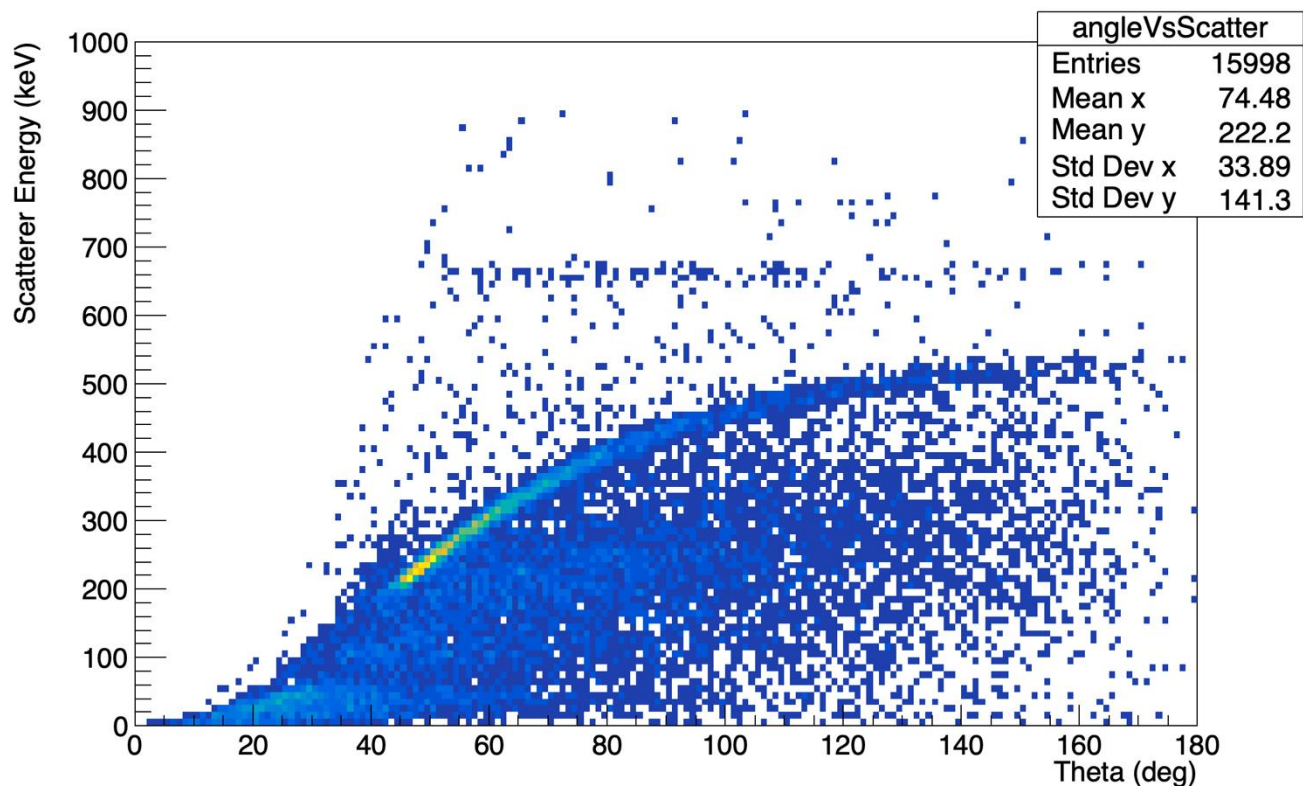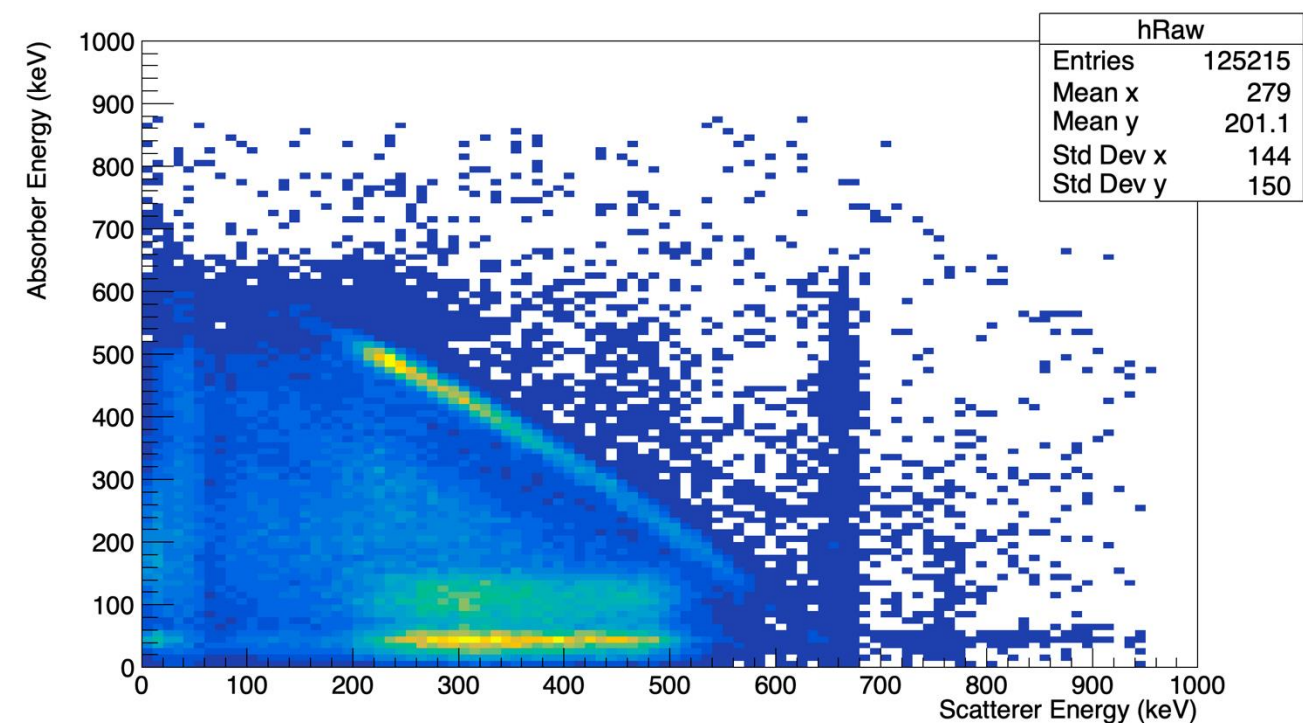
Image Reconstruction Optimisation

The x and y projections (sliced at the maximum y-z and x-z values respectively) of CC1 shown for different numbers of iterations in the Octane EM reconstruction.
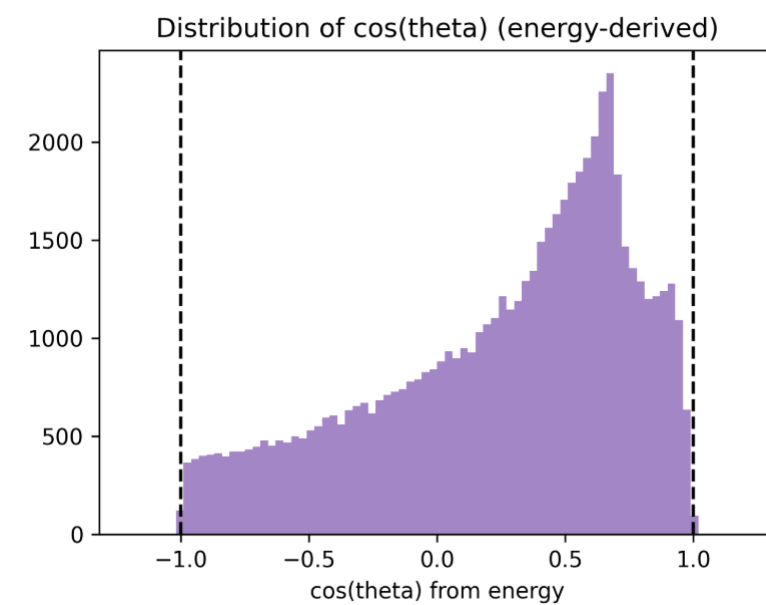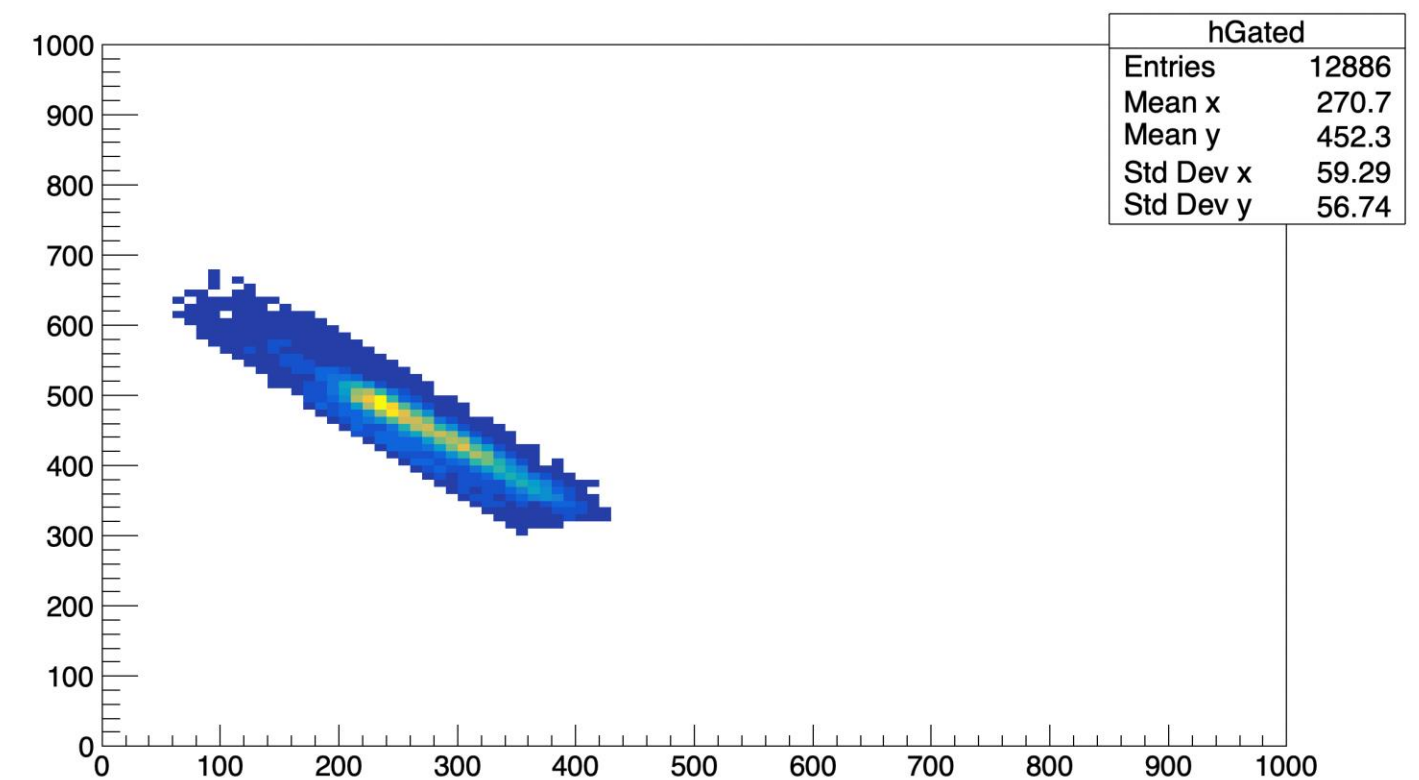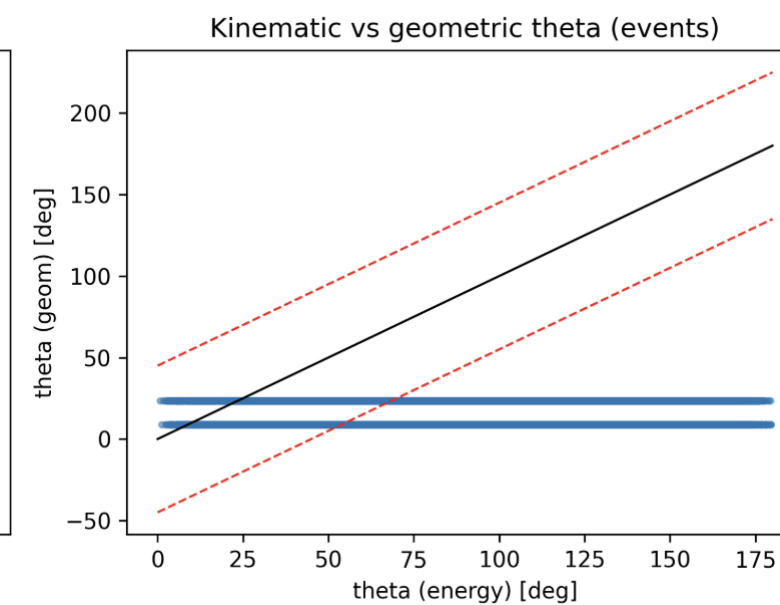
CC Experiment – Source Measurements

Results of 30-min measurement: ^{137}Cs source at (0,0,10) mm from the LaBr$_3$:Ce CC scatterer face

Theta derived from energies (Compton formula) vs theta derived from hit positions (geometrical)

Filtering

Advancing knowledge. Transforming lives. Inspiring a nation.

CC Experiment – Source Measurements

Results of 30-min measurement: ^{137}Cs source at (0,0,10) mm from the LaBr$_3$:Ce CC scatterer face